THICKNESS ANALYSIS OF THIN FILMS BY ENERGY DISPERSIVE X-RAY SPECTROSCOPY

A THESIS SUBMITTED TO
THE GRADUATE SCHOOL OF NATURAL AND APPLIED SCIENCES
OF
MIDDLE EAST TECHNICAL UNIVERSITY

BY

SEDAT CANLI

IN PARTIAL FULLFILMENT OF THE REQUIREMENTS
FOR
THE DEGREE OF MASTER OF SCIENCE
IN
MICRO AND NANOTECHNOLOGY

DECEMBER 2010

Approval of the thesis:

THICKNESS ANALYSIS OF THIN FILMS BY ENERGY DISPERSIVE X-RAY SPECTROSCOPY

submitted by **SEDAT CANLI** in partial fulfillment of the requirements for the degree of **Master of Science in Micro and Nanotechnology Department, Middle East Technical University** by,

Prof. Dr. Canan Özgen
Dean, Graduate School of **Natural and Applied Sciences** _____

Prof. Dr. Mürvet Volkan
Head of Department, **Micro and Nanotechnology** _____

Prof. Dr. Raşit Turan
Supervisor, **Physics Dept., METU** _____

Assist. Prof. Dr. Burcu Akata Kurç
Co-Supervisor, **Micro and Nanotechnology Dept.,** _____

Examining Committee Members:

Prof. Dr. Macit Özenbaş
Metallurgical and Materials Dept., METU _____

Prof. Dr. Raşit Turan
Physics Dept., METU _____

Prof. Dr. Mehmet Parlak
Physics Dept., METU _____

Prof. Dr. Necati Özkan
Central Laboratory, METU _____

Assoc. Prof. Dr. Akif Esendemir
Physics Dept., METU _____

Date: _____

I hereby declare that all information in this document has been obtained and presented in accordance with academic rules and ethical conduct. I also declare that, as required by these rules and conduct, I have fully cited and referenced all material and results that are not original to this work.

Name, Last Name: Sedat Canlı

Signature:

ABSTRACT

THICKNESS DETERMINATION OF THIN FILMS BY ENERGY DISPERSIVE X-RAY SPECTROSCOPY

Canlı, Sedat

M. Sc., Department of Micro and Nanotechnology

Supervisor: Prof. Dr. Raşit Turan

Co-Supervisor: Assist. Prof. Dr. Burcu Akata Kurç

December 2010, 77 pages

EDS is a tool for quantitative and qualitative analysis of the materials. In electron microscopy, the energy of the electrons determines the depth of the region where the X-rays come from. By varying the energy of the electrons, the depth of the region where the X-rays come from can be changed. If a thin film is used as a specimen, different quantitative ratios of the elements for different electron energies can be obtained. Unique thickness of a specific film on a specific substrate gives unique energy-ratio diagram so the thickness of a thin film can be calculated by analyzing the fingerprints of the energy-ratio diagram of the EDS data obtained from the film.

Keywords: SEM, EDS, EDX, thin film, thin film thickness

ÖZ

ENERJİ DAĞILIMI X-IŞINI SPEKTROSKOPİSİ YÖNTEMİYLE İNCE FİLM KALINLIK ANALİZİ

Canlı, Sedat
Yüksek Lisans, Mikro ve Nanoteknoloji Bölümü
Tez Yöneticisi : Prof. Dr. Raşit Turan
Ortak Tez Yöneticisi: Yrd. Doç. Dr. Burcu Akata Kurç

Aralık 2010, 77 sayfa

EDS, malzemelerin nitelik ve nicelik analizini yapan bir araçtır. Elektron mikroskopisinde, elektronların enerjisi, örnekten gelen X ışınlarının geldiği bölgenin derinliğini belirler. Elektronların enerjileri değiştirilerek, X ışınlarının geldiği derinlik de değiştirilebilir. Herhangi bir ince film yapısı incelendiğinde, farklı elektron enerjilerinde farklı element yüzdeleri ile karşılaşılır. Belirli bir filmin, belirli bir kalınlığı, kendine özgü bir enerji-oran diagrami verecektir ki, biz bu diagramı o filmin o kalınlığı için parmakizi olarak nitelendirebiliriz ve buradan filmin kalınlığına ulaşılabilir.

Anahtar Kelimeler: SEM, EDS, EDX, ince film, ince film kalınlığı

To my grandfather,

ACKNOWLEDGEMENTS

First of all, I would like to express my gratitude to my supervisor Prof. Dr. Raşit Turan, for having provided me excellent working conditions, encouragement and guidance throughout this study. I could summarize my feelings as: “If you have chance to work with him don’t miss it.”

I would like to thank my committee members Prof. Dr. Macit Özenbaş, Prof. Dr. Mehmet Parlak, Prof. Dr. Necati Özkan and Assoc. Prof. Dr. Akif Esendemir for their time and helpful comments.

I want to thank to my present and former group partners Selçuk Yerci, Umut Bostancı, İlker Yıldız, Arife İmer, Ayşe Seyhan, Seda Bilgi, Nader A. P. Moghaddam, Urcan Güler, Döndü Şahin, Buket Kaleli, Fırat Es, Mehmet Karaman, Olgu Demircioğlu, İrem Tanyeli, Kutlu Kutluer. I would especially like to thank to Mustafa Kulakçı for his great help in thermal evaporator system, for his great jokes and great personality, I also want to thank to the manager of Central Laboratory, Prof. Dr. Hayrettin Yücel and vice president of METU, Prof. Dr. Çiğdem Erçelebi for their support.

I would like to thank to my work friends who studied with me and gaining motivation to me: Burcu Akata Kurç, Leyla Molu, Ayşe Eda Aksoy, Özgür Erişen, Kaan Kirdeciler, Sezin Galioğlu, Esin Soy, Berna Kasap, Levent Yıldız, Uğur Özgürgil . I would like thank to İlker Doğan and Hasan Başar Şık for being my best friends for long years, to my sister Seda Canlı for her help, to my family for their patience to me during this study and most especially to Demet Kaya for her greatfull support.

Finally my special thanks goes to Seçkin Öztürk for his brainstorming performance in this study and for his great friendship.

TABLE OF CONTENTS

LIST OF TABLES

TABLES

LIST OF FIGURES

FIGURES

LIST OF ABBREVIATIONS

A : absorption coefficient

BSE : back-scattered electrons

CASINO : monte **Ca**rlo **Si**mulation of electro**n** Trajectory in S**o**lids

CIGS : Copper Inidium Galium Selenide

CL : cathodoluminescence

DC : direct current

EAR : EDS Atomic Ratio

EDS : Energy Dispersive X-ray Spectroscopy

EPMA: Electron Probe Micro Analyzer

F : fluorescence coefficient

ITO : Indium Tin Oxide

LCD : liquid crystal displays

Lsec : Live seconds (total spectrum collection time)

MEMS : microelectromechanical systems

MOCVD : metal-organic chemical vapor deposition

MOS : Metal Oxide Semiconductor

MOS-FET : Metal oxide semiconductor field effect transistor

p-i-n : p-type, intrinsic, n-type

PV : photovoltaic

PVD : Phisical Vapour Deposition

RF : radio frequencySE : Secondary electrons

SEM : scanning electron microscope

TEM : transmission electron microscopes

TFT : Thin Film Transistor

XRD : X-ray diffraction

XRF : X-ray fluorescence

Z : atomic number coefficient

CHAPTER 1

INTRODUCTION

1.1 Thin Films in Nanotechnology

Nanotechnology generally deals with technologies utilizing new functionalities of materials at nanoscale, which is in the range of 1 billionth of a meter. It covers fields from physics to chemistry, biology to material science, electronics to textile engineering, chemical engineering to even mechanical engineering and can include development in a variety of specialties. Thin films are widely used in nanotechnology. Optical coatings, antibacterial surfaces, ferromagnetic films in memory applications, thin film transistors in liquid crystal displays, even new generation solar cells are some examples of applications of thin films in industry at nanoscale.

A thin film is a material created ab initio by the random processes of nucleation and/or growth of individual condensing / reactive atom / ion / molecules on a substrate. The physical, chemical, metallurgical and structural properties of such material are strongly dependent on a number of deposition and growth parameters and thickness can be controlled by varying these parameters. Thin-film may include a considerable thickness range, varying from a few nanometers up to ten microns [1].

During recent years, new developments in microelectronics, microelectromechanical systems (MEMS), and optoelectronics have created significant opportunities for thin-film materials and silicon technology. Deposition methods of thin films for these applications such as ion beam sputtering, radio frequency (RF) planar magnetron sputtering, direct current (DC) magnetron sputtering, metal-organic chemical vapor deposition (MOCVD) have been developed and improved for these new applications. On the other hand variations in the thickness of the fabricated thin films have become important as the dimensions of the systems have shrunk with nanotechnology applications. Consequently, the thickness measurements have become crucial for the establishment of reliable thin film production [2]. Material's mechanical, magnetic and electrical properties such as strength, conductance, permiability are all related to the thickness of the film. It is thus very important to measure the thickness of the films with high accuracy [3] .

One of the usage of thin films in nanotechnology is in photovoltaic applications. A photovoltaic (PV) cell is a device which converts energy of light coming from sun, directly into electrical energy by means of photovoltaic effect. The structure of a photovoltaic cell is composed of thin layers of conductive, semiconductive and insulator materials. In the active part of the PV cell p and n type semiconductors form a junction which is used to collect the generated electron-hole pairs. Nowadays, in order to reduce the cost of the electricity generation, various thin film systems such as amorphous Si, Cadmium Telluride (CdTe), Copper Inidium Galium Selenide (CIGS) are used as a semiconductor in PV applications. Indium Tin Oxide (ITO) is optically transparent but electrically conductive layer and glass is the main substrate of PV structure. The thickness of the layers are critical because of efficiency [4]. A few nanometer change in the thickness of the layers may result in decrease in the efficiency of the structure. These applications require precise fabrication and characterzation of thin films.

Another application of thin films is in the Thin Film Transistor (TFT) and Metal Oxide Semiconductor (MOS) technology. TFT is a kind of field effect transistor fabricated by deposition of a semiconductor and dielectric layer on a supporting substrate with metalic contacts. The primary application of TFT is in liquid crystal displays (LCD). ZnO is mainly used as a thin film in TFT structures because it is above 80% transparent at visible range and it has high field effect mobility. In addition, thin thermal oxide layer is grown on the substrate as an insulator [5]. Metal oxide semiconductor field effect transistor(MOS-FET) structure is a kind of transistor in which a voltage applied to the oxide-insulated gate electrode can induce a conducting channel between the two other contacts called source and drain [6]. Oxide-insulated gate thickness is fundamental for transistor performance because it is a capacitor and thickness affects the capacitance.

1.2 Thickness Measurements of Thin Films

The thicknesses of thin films vary from few nanometers to tens of microns. For different type and thickness of films, there are different methods for measurement. For example, if an optically transparent thin film on an opaque substrate is to be measured, one of optical thickness measurement techniques such as ellipsometry can be used. If the sample is not optically transparent, and there are steps on the surface, the best way for measuring the thickness is scanning probe microscopy. For such samples, profilometer is also another method for measuring the thickness. Each measuring method has some advantages and disadvantages. For example if the thin film is not optically transparent, ellipsometry cannot be used or if there are not any steps on the film, atomic force microscope or profilometer is not a suitable tool for the measurement.

Measurement limits are different for different methods. Optical techniques are more precise than other techniques. For an optical method, multiple beam interferometer, the resolution is nearly 1 Angstrom and upper limit is at the range of the wavelength (around 400 nm) [7]. The higher resolution capability comes from the interferometric sensitivity of the system. At a specific wavelength, LASER beam is deflected on the sample. The reflected beam from the surface of the coating and from the interface of the coating and the substrate, construct interference on the detector and interfaced light is analyzed for thickness determination.

Mechanical thickness determination techniques are not as sensitive as optical methods. Mainly, a sharpened tip is used for linearly scanning the surface and the vibration frequency of the cantilever is analyzed for the thickness of the step. The position of the cantilever is determined by an optical method: reflecting laser beam spots on the detector and it detects the position of the beam. Still the accuracy of this method is not as high as direct optical methods because of the elasticity and thermal expansion effects of the cantilever.

There are also microscopic methods for thickness measurements. Optical and electron microscopes can be used for direct thickness determination. The disadvantage of these methods is the specimen must be cross-sectional and vertically located. The interface of the substrate and the film must give contrast and the cross-sectional surface must be clean. If all the ideal conditions are satisfied, the resolution limit for thickness measurement is nearly the resolution limit of the microscope system. For optical microscopes, it is 400nm and for scanning electron microscopes, 2 nm and transmission electron microscopes (TEM), the resolution limit is below 1 nm.

In this work we have developed an alternative method for thin film thickness measurement using Energy Dispersive X-ray Spectroscopy (EDS). This new approach is shown to be very powerful and practical in many applications. It provides an easy and reliable determination of the thickness during regular SEM analysis of a thin film system. Below we present the basic principles of this new techniques after giving the necessary background information.

1.3 SEM and EDS

1.3.1 Scanning Electron Microscopy (SEM)

The scanning electron microscope (SEM) is a type of electron microscope that creates images of the sample surface by scanning it with a high-energy electron beam in a raster scan pattern. The electrons interact with the atoms that make up the sample producing secondary electrons, backscattered electrons, x-rays that contain information about the sample's surface topography, composition and other properties such as electrical conductivity.

Figure 1.1: Scanning Electron Microscope with EDS attachment used in this study.

SEM produces secondary electrons, back-scattered electrons (BSE), light (cathodoluminescence), characteristic X-rays, specimen ground current and transmitted electrons by electron material interaction. Mainly all SEMs have secondary electron detectors but single SEM attached with all detector types is rare. The signals are produced by interactions of the electron beam with the atoms at the surface or near the surface of the sample. In the most common or standard detection mode, secondary electron imaging or SEI, the SEM can produce very high-resolution images of a sample surface, revealing details about less than 1 to 5 nm in size. Because of the very narrow electron beam, SEM images have a large depth of focus yielding a characteristic three-dimensional appearance useful for understanding the surface structure and surface topology of a sample.

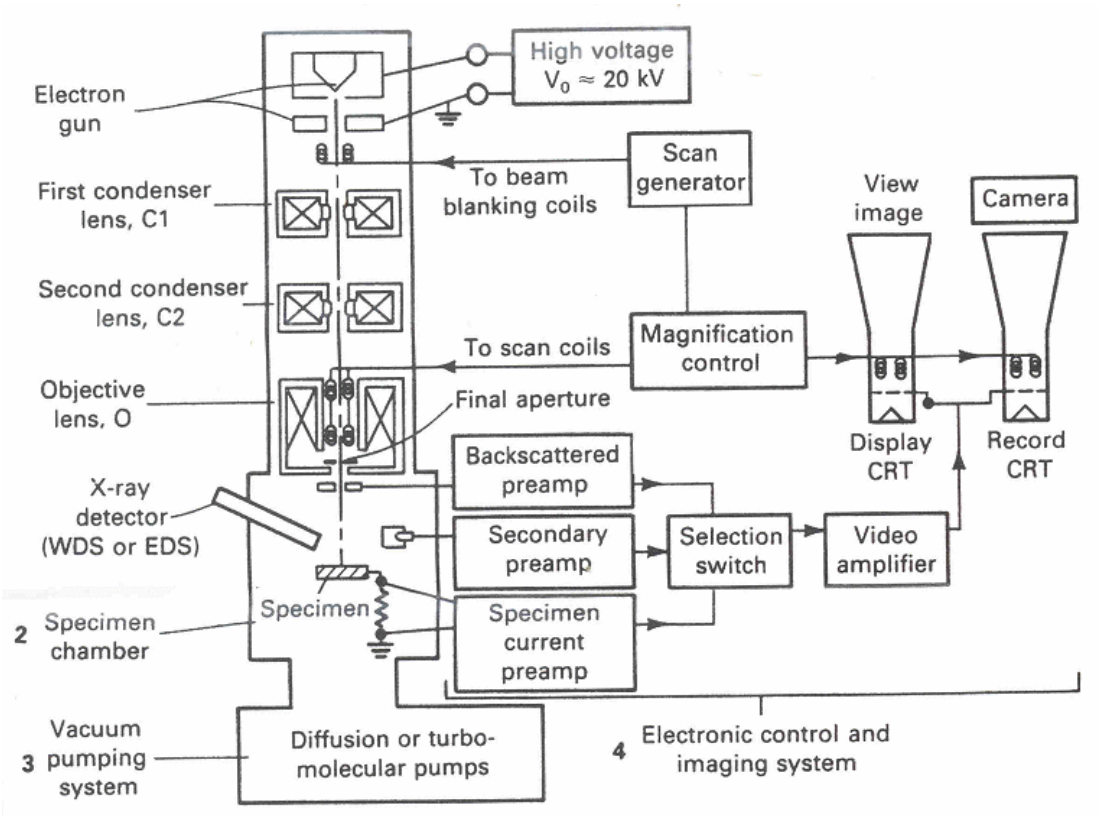

Figure 1.2: Schematic diagram of a typical scanning electron microscope system [8].

In Figure 1.2, schematic diagram of an SEM can be seen. An electron gun is located at the top of the system, which supplies electrons of constant energy through the column. In the column, just after the blanking coils, there are condenser lenses. Objective lenses are located just above the chamber. Scan coils are in the objective lenses. In the chamber, specimen holder and detectors are located. Vacuum pumping system is just below the chamber. The electronic control and imaging system controls all the gun, lenses, stage and detectors and generates the image on a CRT monitor or on a computer.

Scanning Electron Microscopy is widely used for analyzing samples in a nondestructive way. It is very easy process to load the sample into the vacuum

chamber. Then you can continue the analysis by turning the beam on. Almost every solid state sample can be placed into the chamber as a specimen. In the current study, FEI brand, Quanta 400 FEG model SEM is used. It has a very large voltage scale, from 500 Volts to 30kVolts by steps of 1 Volt. The system also has field emission gun, which makes the beam much denser, resulting in brighter images.

1.3.2 Electron Beam- Material Interaction

Accelerated electrons onto a material interact with the atoms of the target specimen or they may pass through the specimen without any interaction. The interaction can be elastic scattering or inelastic scattering. Elastic and inelastic scattering result in such signals which are used for imaging, quantitative and qualitative analysis by generation of x-rays. Secondary electrons (SE), backscattered electrons (BSE), auger electrons, cathodoluminescence (CL) and characteristic X-rays are the typical signals used for imaging and analysis [9]. Quantitative and qualitative analyses of materials as well as element mapping of the surface, typically utilize characteristic X-rays. Bremsstrahlung radiation is a continuous spectrum of X-rays from zero to the energy of the electron beam, and forms a background in which characteristic X-ray must be considered. Further, X-rays generated from a specific target material are used as the roughly fixed-wavelength energy source for X-ray diffraction (XRD) and X-ray fluorescence (XRF) investigations (Figure 1.3).

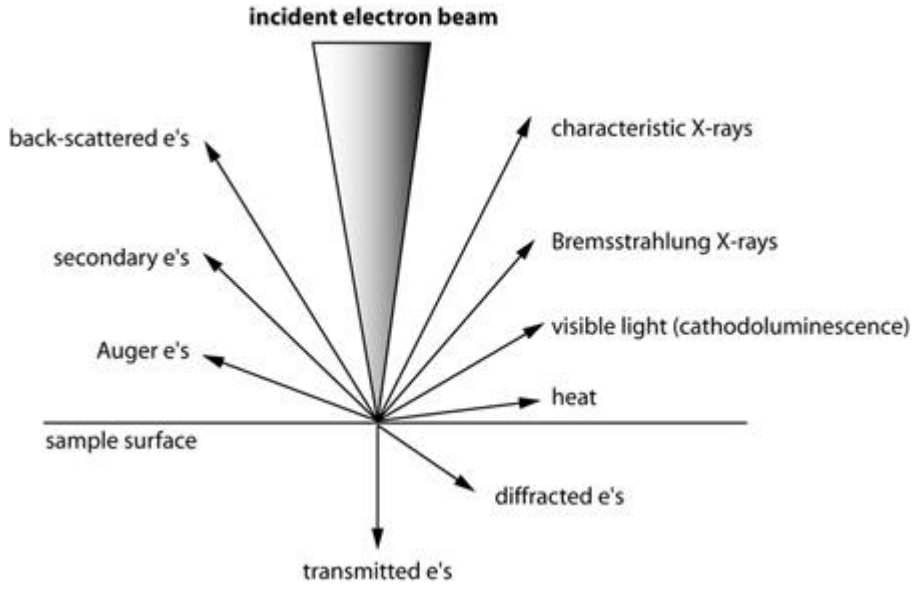

Figure 1.3: Interaction types between electrons and a sample depends on the incident energy of the electron beam, such as auger, secondary and back-scattered electrons, X-rays (characteristic and Bremsstrahlung), light (cathodoluminescence) and heat (phonons) are emitted. Several of these interactions are used for imaging, quantitative and qualitative analysis [10].

Where an electron beam impinges on a sample, electron scattering and photon- and X-ray-production develops in a volume (the electron interaction volume) that is dependent on several factors (Figure 1.4).

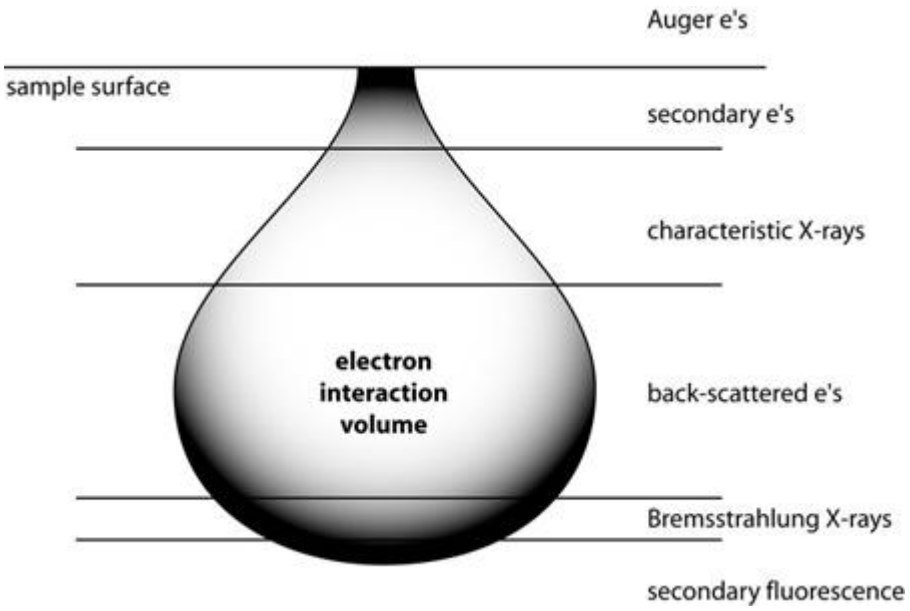

Figure 1.4: Electron interaction volume within a sample. Each of the electron, X-ray and light emissions generated after the impingement of a high-energy electron beam, develops at different depths (volumes) within the sample. In turn, the volume of generation of the emitted energy controls the spatial resolution of the signal.

Each of individual signals used for imaging or X-ray generation is produced from different electron-electron interaction volumes and, thus each of the signals has different imaging or analytical resolution. Auger and Secondary images have the high resolution image quality, generated from the smallest volume near the surface of the sample compare to backscattered electrons in which are generated over a larger volume and with the intermediate image resolution. Cathodoluminescence also generated over the largest volume, even larger than Bremsstrahlung radiation, but image resolution is very poor compare to others.

1.3.3 Energy Dispersive X-ray Spectroscopy (EDS)

One of the most powerful attachments of SEM is Energy Dispersive X-ray Spectroscopy (EDS). Atomic qualitative and quantative information from the specimen can be supplied by an EDS system. It relies on the investigation of a sample through interactions between electromagnetic radiation and matter, analyzing x-rays emitted by the matter in response to being hit with charged particles. Its characterization capabilities are due in large part to the fundamental principle that each element has a unique atomic structure allowing x-rays that are characteristic of an element's atomic structure to be identified uniquely from each other.

1.3.4 EDS Hardware and Operating Principle

An undoped silicon has four outer shell electrons. All of the valance bands are full and next highest available energy levels in the conduction band are empty. There are no excess electrons available for charge transport in the conduction band, and there are no holes in the valence band. Such a material is called an intrinsic semiconductor. It will not conduct current in an applied electric field unless it absorbs energy causing electrons to be promoted into the conduction band, leaving holes behind. For this reason intrinsic semiconductors are used as radiation detectors. In actual practice, silicon is not sufficiently pure to achieve the intrinsic condition. Instead, detector crystals are made to behave like intrinsic silicon by a process. Lithium (an n-type dopant) is applied to the surface of p-type silicon and caused to diffuse into the crystal, forming a p-n junction. While the p-

n junction boundary is an intrinsic semiconductor, it is only a few micrometers thick. However, when a reverse bias is applied to p-n junction at elevated temperature, the intrinsic region can be enlarged to a few millimeters, making it suitable for a detector material after most of the p-type material is removed. Both steps are performed above room temperature, but even at room temperature, Li is mobile in the presence of an applied field. For this reason detectors can never be allowed to operate under bias except near liquid-nitrogen temperatures.

The operating principles of a solid-state detector system are illustrated in Figure 1.5. X-ray photons from the sample pass through a thin window isolating the environment of the specimen chamber from the detector, into a cooled, reverse-bias p-i-n (p-type, intrinsic, n-type) Si(Li) crystal. Absorption of each individual x-ray photon leads to the ejection of a photoelectron, which gives up most of its energy to the formation of electron-hole pairs. They are swept away by the applied bias to form a charge pulse, which is then converted to a voltage pulse by a charge-to-voltage converter (preamplifier). The signal is further amplified by a linear amplifier and finally passed to a computer X-ray analyzer, where the data is displayed as a histogram of intensity by voltage [11].

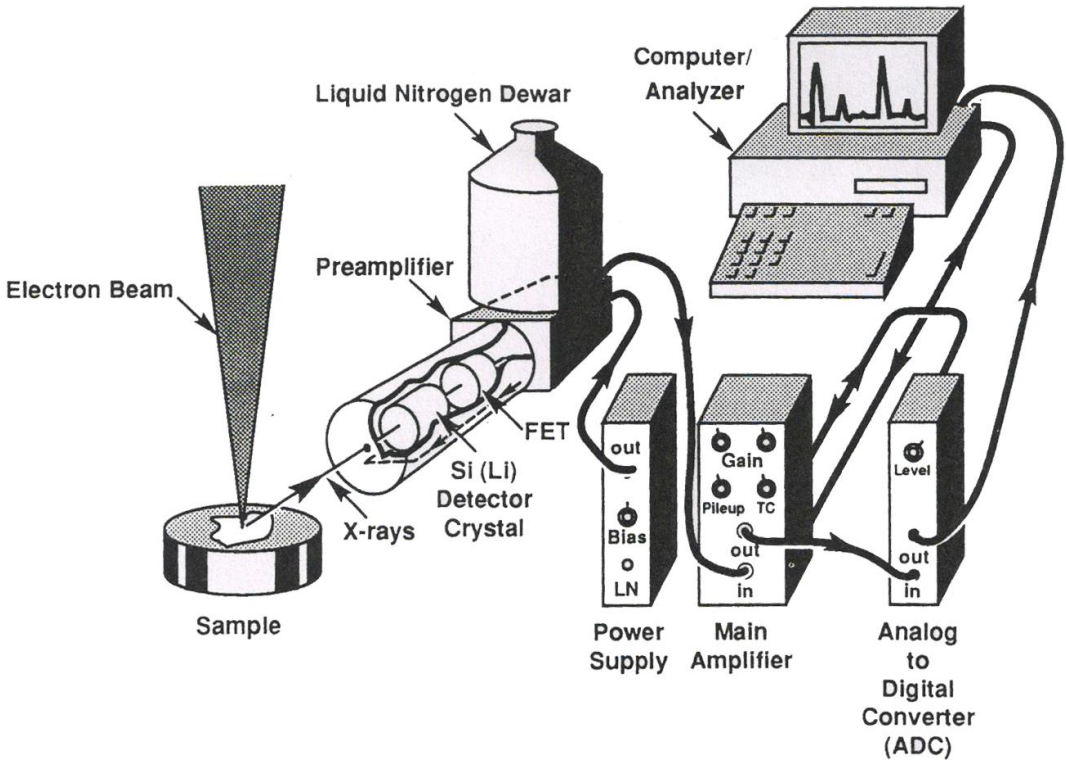

Figure 1.5 Schematic representation of an EDS system and its associated electronics [12].

The typical physical appearance of a detector system can be seen in more detail in Figure 1.6. The lithium doped silicon crystal is mounted on a cold finger connected to a liquid-nitrogen reservoir stored in the dewar. Since the detecting crystal is light sensitive, it is essential to block visible radiation, preferably through the use for an opaque window. Windowless and ultrathin-window EDS can be used if the specimen chamber is light tight and the specimen is not cathodoluminescent. The detector chamber is also sealed under vacuum both to prevent contamination from the specimen region (especially when the specimen chamber is brought to air pressure) and to more easily maintain the low temperature essential for reducing noise.

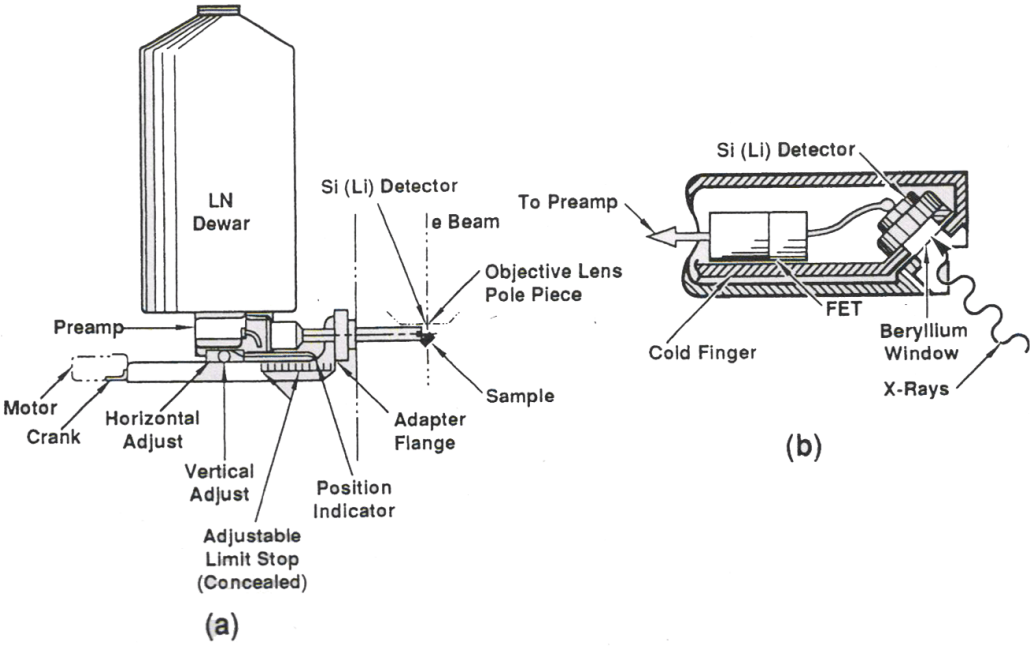

Figure 1.6: (a) Physical appearance of a retractable detector and associated preamplifier electronics. (b) Detail of Si(Li) mounting assembly [12].

1.3.5 Accuracy of EDS

Accuracy of EDS spectrum can be affected by many variants. Window, in front of the SiLi detector can absorb low-energy X-rays (i.e. EDS detectors cannot detect presence of elements with atomic number less than 5, meaning that EDS cannot detect H, He, Li, or Be) [13] [14]. Differing the over-voltage of the EDS will result in different peak sizes - Raising over-voltage on the SEM will shift the spectrum to the larger energies making higher-energy peaks larger while making lower energy peaks smaller. Also many elements will have overlapping peaks (ex. Ti K_β and V $K\alpha$, Mn K_β and Fe K_α). The accuracy of the spectrum can also be affected by the nature of the sample. X-rays can be generated by any atom in the sample that is sufficiently excited by the incoming beam. These X-rays are

emitted in any direction, and so may not all escape the sample. The likelihood of an X-ray escaping the specimen, and thus being available to detect and measure, depends on the energy of the X-ray and the amount and density of material it has to pass through. This can result in reduced accuracy in inhomogeneous and rough samples.

1.3.6 ZAF Correction

The EDS system constructs the spectrum by measuring the energy of the x-rays and counts the number of signals for specific energy. After enough number of counts (around 50000), the spectrum is constructed and the peaks for a specific energy, corresponding to elemental transitions can be easily seen. Y-axis of the graph just gives the number of counts, and cannot be directly used for elemental ratios. The peak values must be normalized by some coefficients to be used for elemental ratios. These coefficients are Z (atomic number coefficient), A (absorption coefficient) and F (fluorescence coefficient).

The number of protons in an atom affects the interaction density of electrons sent to the specimen. Higher atomic number results in more interactions of electrons with the atom. As a result, the number of x-rays coming from the specimen increases with the atomic number of the atom. For this reason, in EDS spectrum, higher atomic number elements give higher counts and this artificial effect must be corrected. Z (atomic number coefficient) is used for this correction.

Another correction coefficient “A” refers to absorption coefficient in EDS measurements. Generated x-rays in the specimen can re-radiate other neighboring atoms and x-ray loses its energy. Because of this reason, x-ray detector cannot

count initial x-ray correctly. Absorption factors in EDS ratios are corrected by a coefficient ‘A’ in EDS measurements.

Compared to Z and A corrections in EDS measurements, F (fluorescence) correction is not so critical, even that, F correction is done in EDS measurements. Similar to A correction, F correction comes from re-radiation of atoms by neighboring atoms’ emitted x-rays.

The use of EDS in thickness determination is the main idea developed during this study. As will be shown below, X-ray generated at different thicknesses can be normalized to determine the thickness of a thin film deposited on a substrate.

1.4 Interaction Volume of Electrons

Probe electrons generate X-Rays as they travel and interact with the substrate atoms. The depth and the paths they follow differ with the substrate density and the energy of the electrons. The relation between the depth, density and the energy can be generalised as follows:

$$Density \times Depth \approx Energy \quad (1)$$

$$\frac{mg}{cm^3} \times cm \approx eV \quad (2)$$

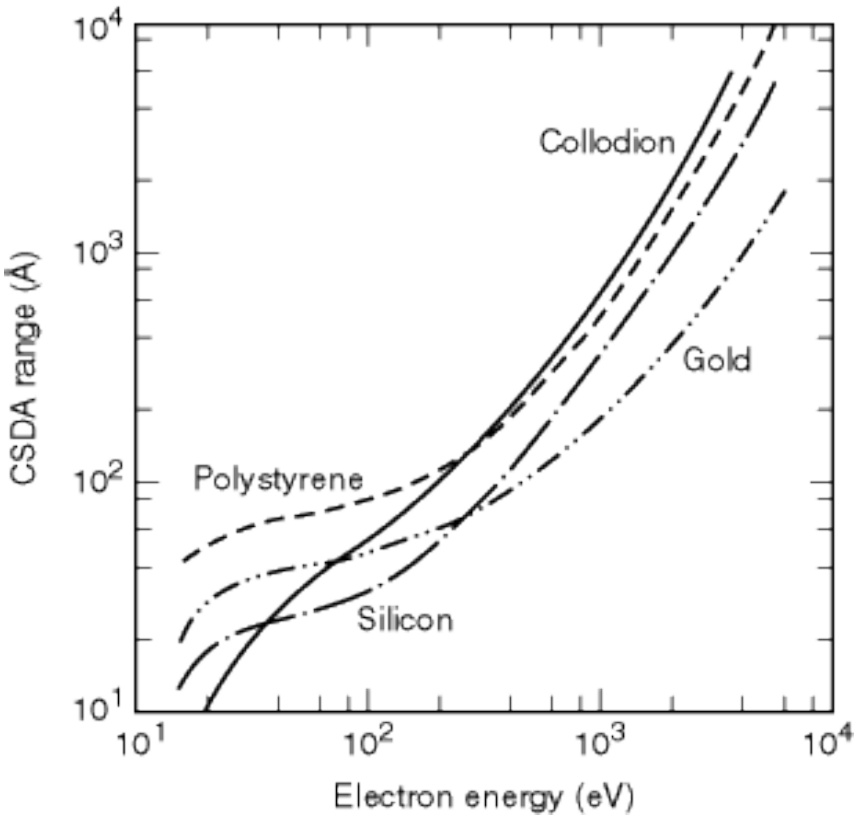

Figure 1.7: Range of electrons vs Electron energy [15]

The general relation can also be seen in the Figure 1.7. The amount of material that the electron can pass through is increases almost linearly with the increasing energy of the electrons. The amount of the material can be defined by the density of the material multiplied by the depth of the electron trajectory. Because of this reason electrons with a fixed energy can go deeper in the materials which are made of lighter elements when compared with the materials made of heavy elements. As can be seen in Figure 1.8, electrons projected with 10 keV energy can penetrate through Si deeper when compared with Au.

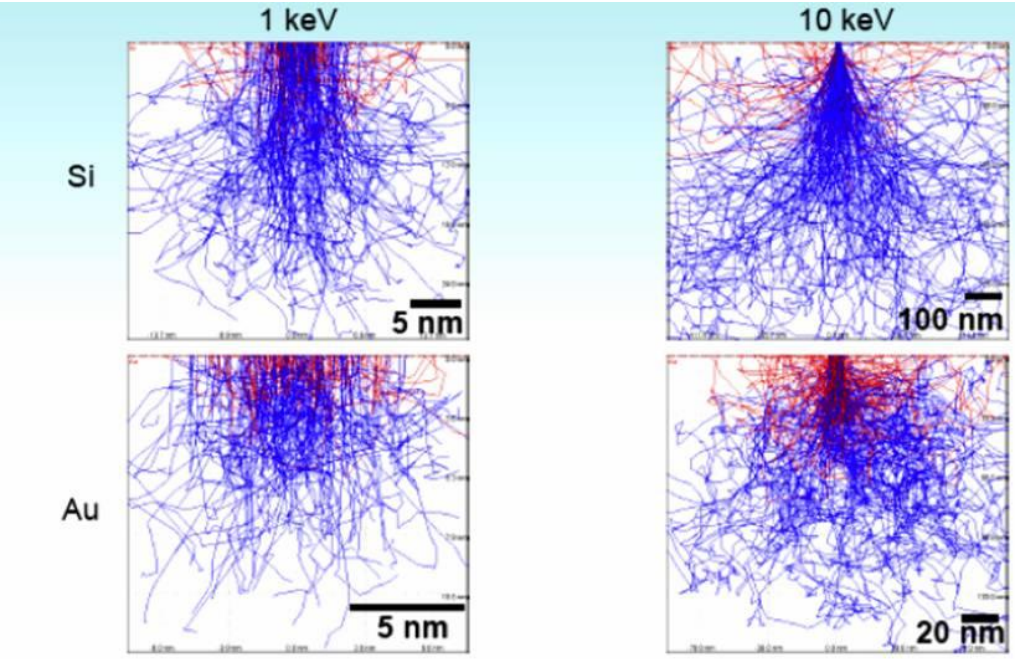

Figure 1.8: Montecarlo electron-trajectory simulations of Si and Au substrates at 1 and 10 keV [10].

As electron penetrates through material, it experiences multiple scatterings while losing some of its energy and generating photons, plasmons, phonons. The travel goes till the electron looses all its energy because of the scatterings. Because of this reason higher energy electrons can penetrate through material deeper when compared with lower energy electrons. This phenomenon is used as the backbone of the study. In Figure 1.9 the effect of the electron energy can be seen. As the electron energy increases the penetration depth and the interaction volume increases while the shape of the interaction volume remains almost the same.

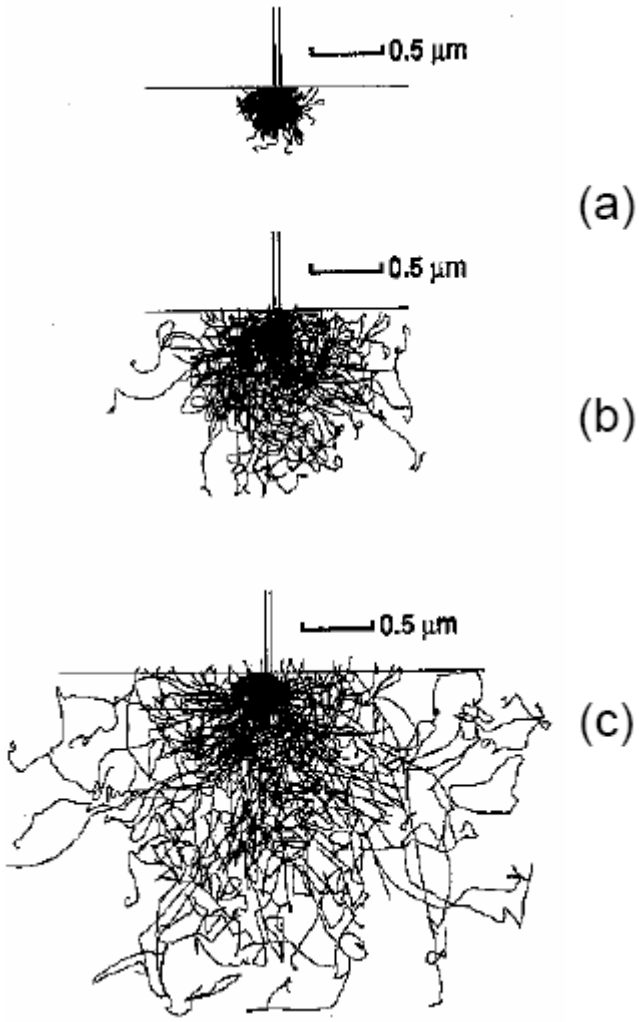

Figure 1.9: Monte Carlo electron-trojectory simulations of the interaction volume in Fe at a) 10 keV , b) 20 keV, c) 30 keV [12]

1.5 Similar Studies in Literature

In literature, there are similar studies to this study. Most of them are done using scanning electron microscope or electron microprobe. The EDS results are given and it is shown that, thickness determination can be done using EDS results of different energy of incident electrons. The fabrication methods of the samples show some similarities to this study.

There is a also commercial software developed for thickness measurements of thin films by EDS.

These studies along with similarities and differences between them and the present study are summarized below.

1.5.1 Thickness Determination of Copper by Electron Probe Microanalyzer

Characterization of thin films on substrates includes both, the determination of the composition as well as the film thickness. In a study reported by Möller et al., both parameters can be deduced from experimental k-ratios in Electron Probe Micro Analyzer (EPMA) [12] [16] . X-ray depth distribution function ϕ (ρz) is defined and used for accurate determination of layer thicknesses [17] [18].

Cu films are deposited by Physical Vapor Deposition (PVD) with deposition rates of 0.01nm-0.1nm/second in Möller's study [19]. Oscillating quartz crystal is used for continuously monitoring the thickness during sample preparation. Profilometer measurements was carried out to check the sample preparation procedure and to obtain a rough estimate of the layer thicknesses.

All analyses were carried out with an electron microscope using wavelength dispersive techniques. Accelerating voltage was varied between 6 and 30kV. Pure Cu and pure Si standards were used. Accuracy of the accelerating voltage was 100V in the voltage range of 8 to 20kV. Moreover Secondary Ion Mass Spectroscopy (SIMS) and Rutherford Backscattering Spectroscopy (RBS) measurements were also performed on the samples.

For four different nominal values, 100 nm 180 nm 270 nm 450 nm, thicknesses are calculated by using EPMA results. The results can be seen in Table 1.1.

Table 1.1: Layer thicknesses determined by EPMA [19]

Electron energy [keV]	X-ray line	Nominal value 100 nm	Nominal value 180 nm	Nominal value 270 nm	Nominal value 450 nm
6	Kα	–	–	–	–
	Lα	108 ± 1	–	108 ± 1	–
8	Kα	–	–	–	–
	Lα	108 ± 1	–	183 ± 2	–
10	Kα	84 ± 1	137 ± 1	59 ± 1	530 ± 5
	Lα	108 ± 1	185 ± 2	237 ± 2	345 ± 3
15	Kα	104 ± 1	186 ± 2	268 ± 3	429 ± 4
	Lα	111 ± 1	185 ± 2	270 ± 3	428 ± 4
20	Kα	101 ± 1	179 ± 2	286 ± 3	471 ± 5
	Lα	112 ± 1	192 ± 2	278 ± 3	453 ± 5
25	Kα	103 ± 1	179 ± 2	280 ± 3	468 ± 5
	Lα	110 ± 1	194 ± 2	284 ± 3	453 ± 5
29	Kα	–	180 ± 2	–	463 ± 5
	Lα	–	197 ± 2	–	470 ± 5
30	Kα	104 ± 1	–	281 ± 1	–
	Lα	105 ± 1	–	283 ± 3	–
all	Kα	102 ± 1	180 ± 2	280 ± 3	466 ± 5
	Lα	109 ± 1	191 ± 2	280 ± 3	454 ± 5

1.5.2 Thickness Determination of FeCoSiB films by EDS

In the work reported by Zhuang, EDS X-ray peak of the thin film to one of substrate at different accelerate voltage; the relation of intensity ratio of I_s/I_f with electron energy is used for determining the thickness of the film [20]. FeCoSiB film is used on glass subsarte. For verfication of the results, profilometer is used. FeCoSiB thin films deposited on commercially available glass by DC magnetron sputter from a bulk material with a composition of 67%Fe, 8%Co, 12%Si and 13%B (At%) for different sputter time. EDS measurements are done by using the voltage range of 5keV to 30keV. Instead of spot analysis, a magnification of 100X is used. In Figure 1.10 show the relation of intensity I_{Si} K_α/I_{Fe} L_α, with electron energy for different thickness of FeCoSiB thin films. For different thickness of thin films, the same trend is observed.

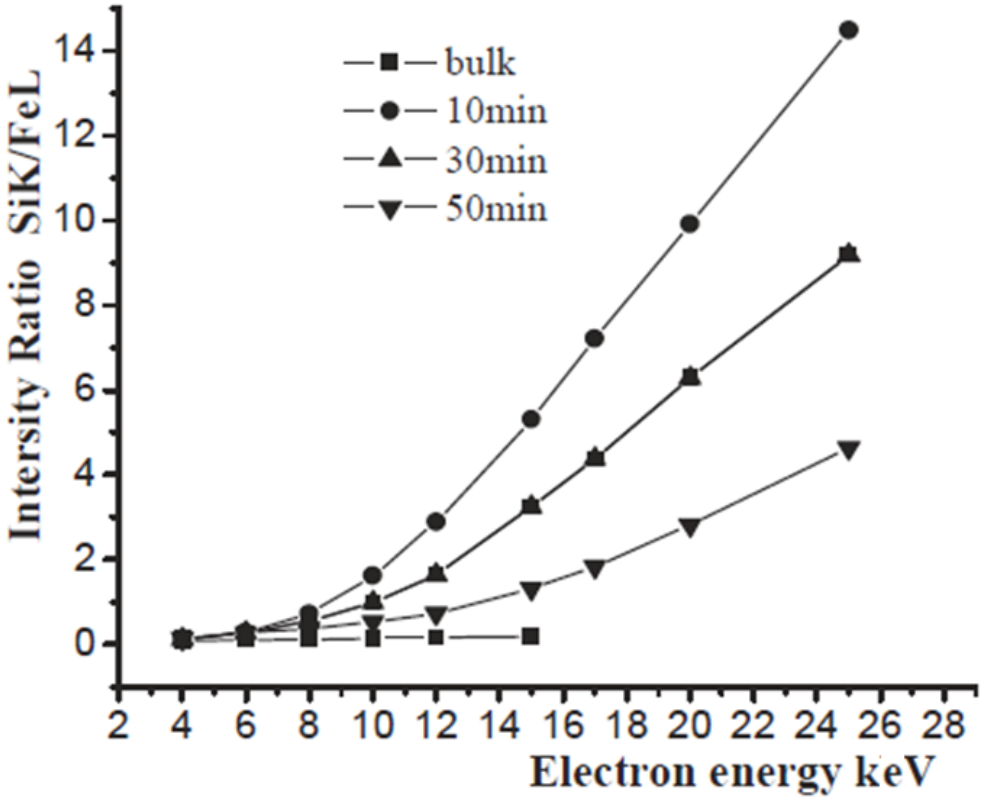

Figure 1.10: Intensity of the substrate and the film with electron energy [20]

Another thickness measurement of metallic thin films work is performed by F.L. Ng [21]. In this study, (EDS) was used to explore the application of X-ray microanalysis in depth determination of metallic films. Al, Ni, Au single-layered films and Au/Ni double-layered film were deposited on silicon (Si) substrate by magnetron sputtering method. Incremental electron beam energy ranging from 4 keV to 30 keV was applied while other parameters were kept constant to determine the electron beam energy required to penetrate the films. Based on the experimental results, the mathematical models for Al, Ni and Au films were established. The effects of probe current at a fixed electron beam energy on the penetration depth were investigated too. The specimen interaction volume was simulated by Monte Carlo program and the simulation results are in good agreement with the experimental results. In Figure 1.11, Aluminium results can be seen.

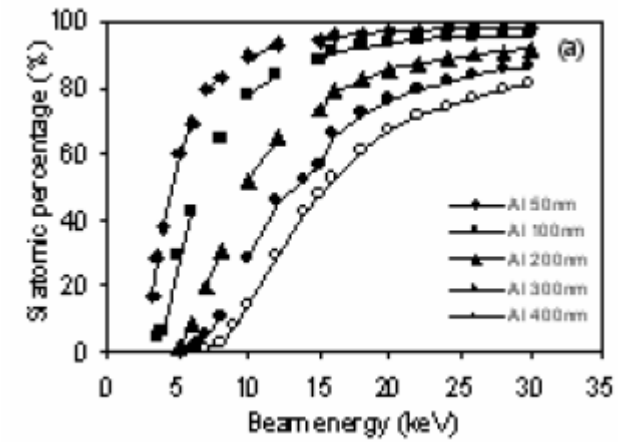

Figure 1.11: Si atomic percentage as a function of electron beam energy for Aluminium film [21].

Moreover, the effect of probe current to the EDS ratios is investigated. In the Figure 1.12, it is seen that there is no any significant effect of probe current to EDS ratios.

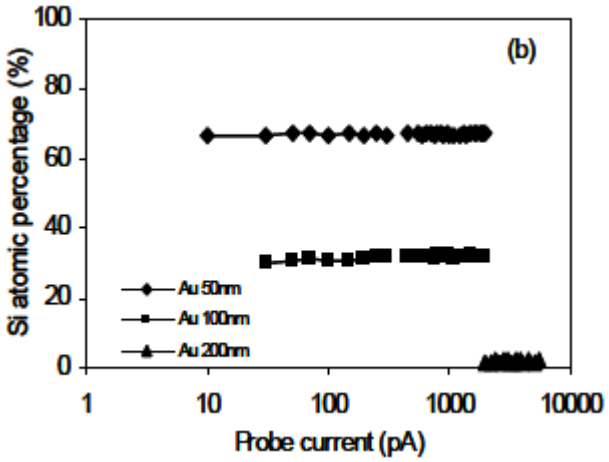

Figure 1.12: Si atomic percentage as a function of probe current for different Au film thicknesses [21].

.

1.5.3 ThinFilmID Software

Oxford Instruments have developed a software named 'Thin Film ID' for determining in-situ composition and thickness of thin film structures [22]. The software is capable to measure from 2nm to 1000 nm thickness, from a 200 nm lateral resolution. The software requires structure and elements definition before run. It can calculate up to 7 layers and upto 16 elements. The thickness calculation method is a trade secret and it works only Oxford brand EDS Systems.

In Sempf's work [23], multilayers of ZrO_2 and TiO_2 on Si substrate is analyzed. In Table 1.2, weight and atomic ratio of elements, density of layers, calculated thicknesses and deviation of the analysis is given for each layer.

Table 1.2: EDX analysis of TiO_2,ZrO_2 multilayers on Si substrate with ThinFilmID [23].

Sample Description:						
Layer	Element	Weight%	Atomic%	Density(g/cm3)	Thickness(nm)	Sigma(nm)
- TiO_2	Ti	59.95	33.33	4.23	10.29	0.79
	O	40.05	66.67			
- ZrO_2	Zr O_2	74.03	33.33	5.68	9.85	0.84
	O	25.97	66.67			
Substrate	Si	100	100			

1.6 Comparison of the Thesis and Literature

In literature, similar studies exist in the field of both electron microprobe and scanning electron microscope. In the current thesis, scanning electron microscope is used. Sample fabrication of the reference studies are done by PVD by Möller,

DC magnetron sputtering by Zhuang, and by Ng. On the other hand, in this thesis, thermal evaporation and wet oxidation methods are used for sample fabrication.

The result verifications are done in Möller's study by SIMS, which is not a right tool for thickness determination. The sputter rate in SIMS is not precise enough to determine the thickness. Profilometer is used for verification of the thicknesses in Zhuang's study. In Ng's study, only some simulated results are used for the verification. Sempf's result verification is done by ellipsometry and electron microscope imaging of the thin film. On the other hand, in this thesis, all possible verification methods are used: profilometer, monte carlo simulation, ellipsometer measurements and electron microscope imaging.

All substrates in the literature related with this field were Si wafer. In this study, Si wafer was used as well. Möller et al. used copper, Zhuang et al. used FeCoSiB, Ng et al. used Al, Ni ,Au and Sempf et al. used ZrO_2 and TiO_2 as thin films on the substrates. Elemental film usage is an advantage for EDS measurements so elemental films were preferred in this thesis.

The EDS results in Möller's study, k-ratios of the elements are used. K-ratio is the raw EDS data which is the x-ray count ratio of the interested element to bulk pure reference at the same analyzing parameters. Using k-ratios in EDS is an old and rough method. In this thesis, instead of k-ratios, elemental atomic ratios of the elements which are obtained after ZAF corrections are used. For different X-ray lines, Kα and Lα, calculation gives different results. For that reason, ZAF correction is needed to get higher accuracy results.

In Zhuang's study, the results are also represented in the ratio of intensities: SiKα, Fe Lα. On the film (at lower voltages) the ratio seems to be constant but at higher voltages,the ratio varies. The calculated thicknesses from that relation by using Sewell's formula are compared with profilometer results and it is seen that the difference is about 10%. For that reason, this method is not good enough for higher accuracy results.

In Ng’s study, the results only show us the critical voltage for the film differs for different thicknesses. There is not any thickness calculation done in this study. Ng only gives atomic ratio&electron voltage curves for Al Ni and Au films and it is shown that probe current does not effect the results. On the other hand, in this thesis, Ge films are also investigated and a thickness calculation method with the atomic ratio&electron voltage curve is introduced.

Sempf only used ThinFilmID in his study, however the film thickness calculation method of ThinFilmID software is not open to public. So calculation methods of ThinFilmID and in the one used in the current thesis are not comparable with each other.

CHAPTER 2

SAMPLE PREPARATION

2.1 Sample Sets

The main goal of sample preparation process is to create uniform and homogeneous thin films on substrates. Silicon wafers coated with thin films are widely used in industry so the main substrate of this work is silicon wafer (110). As examples of thin films, gold, germanium and aluminum are used for different thicknesses. Moreover silicon substrate is oxidized to grow silicon dioxide thin film. For each material, films at 8 different thicknesses are fabricated. Detailed sample sets can be seen in Table 2.1. For gold and germanium, maximum thickness is about 200 nm however for aluminum and silicon dioxide, it is 400 nm because of the reason that density of aluminum and silicon dioxide are lower than gold and germanium. Interaction volume of electrons decreases with density because the mean free path of electrons is very short in higher density materials.

Table 2.1 : Sample Sets

Material (Set Name)	Thickness	Production Method
Gold (B1-B8)	B1 25nm B2 50 nm B3 75 nm B4 100 nm B5 125 nm B6 150 nm B7 175 nm B8 200 nm	Thermal Evaporation on Si wafer
Germanium (C1-C8)	C1 25nm C2 50 nm C3 75 nm C4 100 nm C5 125 nm C6 150 nm C7 175 nm C8 200 nm	Thermal Evaporation on Si wafer
Aluminum (D1-D8)	D1 50 nm D2 100 nm D3 150 nm D4 200 nm D5 250 nm D6 300 nm D7 350 nm D8 400 nm	Thermal Evaporation on Si wafer
Silicon Dioxide (E1-E8)	E1 50 nm E2 100 nm E3 150 nm E4 200 nm E5 250 nm E6 300 nm E7 350 nm E8 400 nm	Wet Oxidation of Si wafer

The silicon dioxide films are produced by wet oxidation method. The thickness of oxide films vary from 50 nm to 400 nm by steps of 50 nm. It can be seen in the Figure 2.1 that for different thickness of oxide are at different colors.

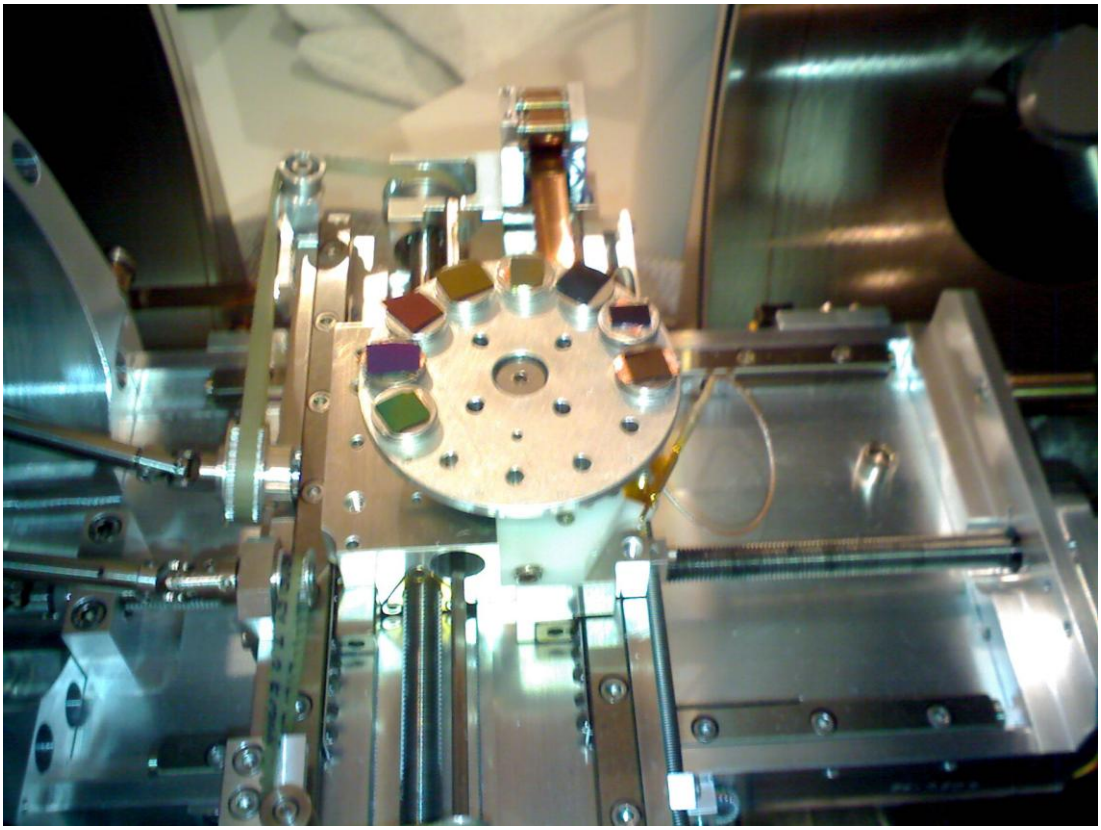

Figure 2.1: Silicon dioxide samples in SEM chamber

2.2 Thermal Evaporation

Thermal evaporation is a method for coating most of materials on substrates. At higher temperatures, with the effect of low pressure, heated coating material evaporates in the chamber. Then the material is deposited onto the substrate. In this study, a home-made thermal evaporation system, which heats tungsten holding boat by the potential up to 120 volts is used. Simultaneously, real-time thickness of the deposited film is measured by using a vibrating crystal thickness monitor system. In the Figure 2.2, a schematic diagram of the system can be seen.

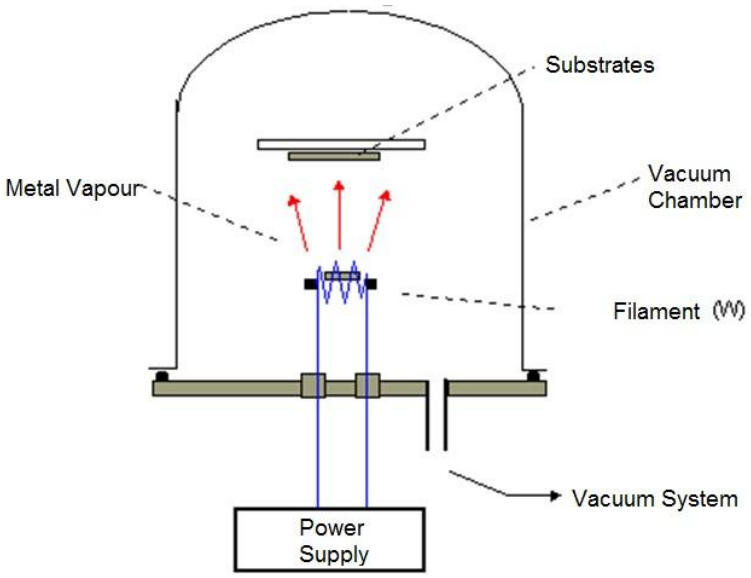

Figure 2.2: Schematic view of thermal evaporation system diagram

There were 8 samples for each sample set so coating together all the samples in the set at the same time would be better for time saving and after each step of coating (25 nm for gold and germanium, 50 nm for aluminum) one sample was taken out from the chamber. Then in the next cycles, thicker samples were coated. After 8th cycle, 8 samples with different thickness for each set were fabricated.

2.3 Wet Oxidation

Silicon Dioxide is widely used insulator material in electronics industry. All of the electronic chips include silicon dioxide inside. Production method of oxide is very important because of the requirements for the quality of the insulators in the industry . Compared to wet thermal oxidation, dry thermal oxidation method results in higher quality films but the process is much slower than wet oxidation (growing 400nm film need over 10 hours) [24]. Because of that reason, wet oxidation method is used in the experiments. The temperature is also critical for growth process. 1000º C is more controllable than higher temperatures so all wet oxidation fabrications are done at 1000º C.

Figure 2.3 : Wet oxidation furnace used in experiments.

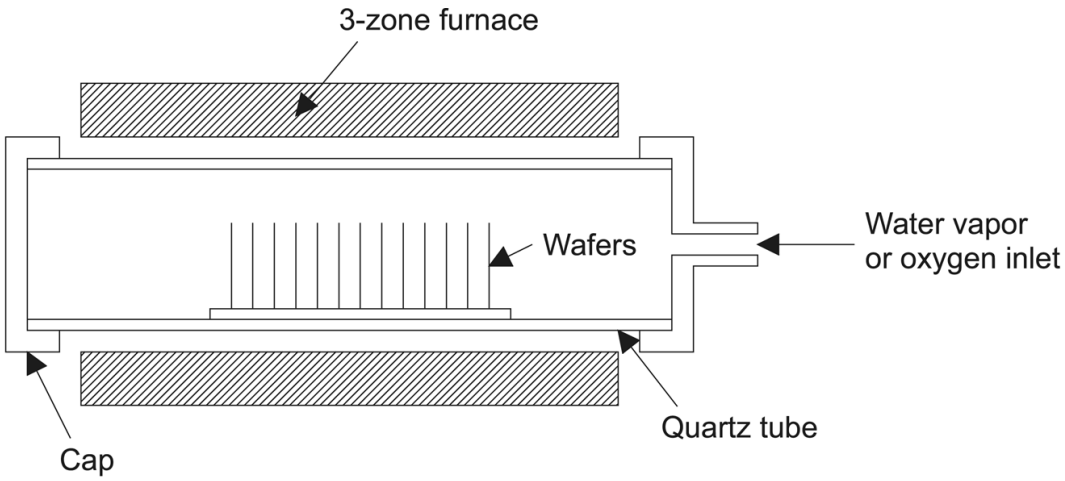

Figure 2.4: Typical oxidation system diagram

The furnace which can be seen in the Figure 2.3 is made up of a quartz tube with a length of 160 cm and a diameter of 13cm. There are covers at both sides of the tube and there are holes on each cover which enables air flow inside. One of these holes is connected to a water boiling system like a hubble-bubble which nitrogen gas pass through inside. The carrier gas nitrogen, carries boiling water to inside the quartz tube. The flow rate of nitrogen is fixed to 2 liters/minute which is an optimized value for the system before. The schematic diagram of the system can be seen in Figure 2.4.

The oxidation process starts from the surface of silicon to inner depths. The oxidation rate is maximum at the beginning and decreases with the time due to the thickness of SiO_2 layer formed at the surface which increases time for oxygen atoms to reach the underlying Si substrate.

During growth process, controlling the thickness is very sensitive to time of the process. Even seconds are very important for thinner samples because of the logarithmic growth rate. In the Table 2.2, it is seen that how the required time varies with specific growth thickness of the silicon dioxide layer [25]. Detailed oxide growth rate chart for dry and wet oxidation at different temperatures can be found in Appendix A.

Table 2.2: Wet oxidation growth time for different thicknesses at 1000º C.

Oxide Thickness (nm)	Oxidation Time (hour:minute:second)
50	0:04:22
100	0:09:46
150	0:16:06
200	0:23:23
250	0:31:37
300	0:40:47
350	0:50:55
400	1:01:58

CHAPTER 3

CHARACTERIZATION

The characterizations of the samples are done by various diagnostic tools. The main goal of this study is related with EDS so the main characterization studies were mainly carried out via EDS attached to the SEM. Other characterization techniques during the study were used for thickness verification of the thin films. These methods can be listed as mechanical characterization and optical thickness measurements, which were done by using profilometer and ellipsometer equipments.

3.1 Profilometer Measurements

Profilometer is a tool for measuring height of surface structures on a substrate. It is a mechanical characterization tool. As seen in Figure 3.1 , a tip is used as a probe which is attached just below a cantilever. A laser beam is reflected from the top side of the cantilever to an optical detector. Optical detector is generally a line array CCD which detects the laser beam reflected from the cantilever. The probe linearly scans the surface and reflected beam from the top surface of the probe is analyzed for determining the height difference of the structure and substrate. The probe is specially designed for very accurate measurements in vertical axis (at the range of 1 nm) and it scans thru the sample in one direction by moving the sample stage. The sample is put on a stage which is movable in x and y axis. The system

is controlled by computer software where an optical microscope is used for fine alignment. The computer software interface which gives thickness of the steps on the sample can be seen in Figure 3.2.

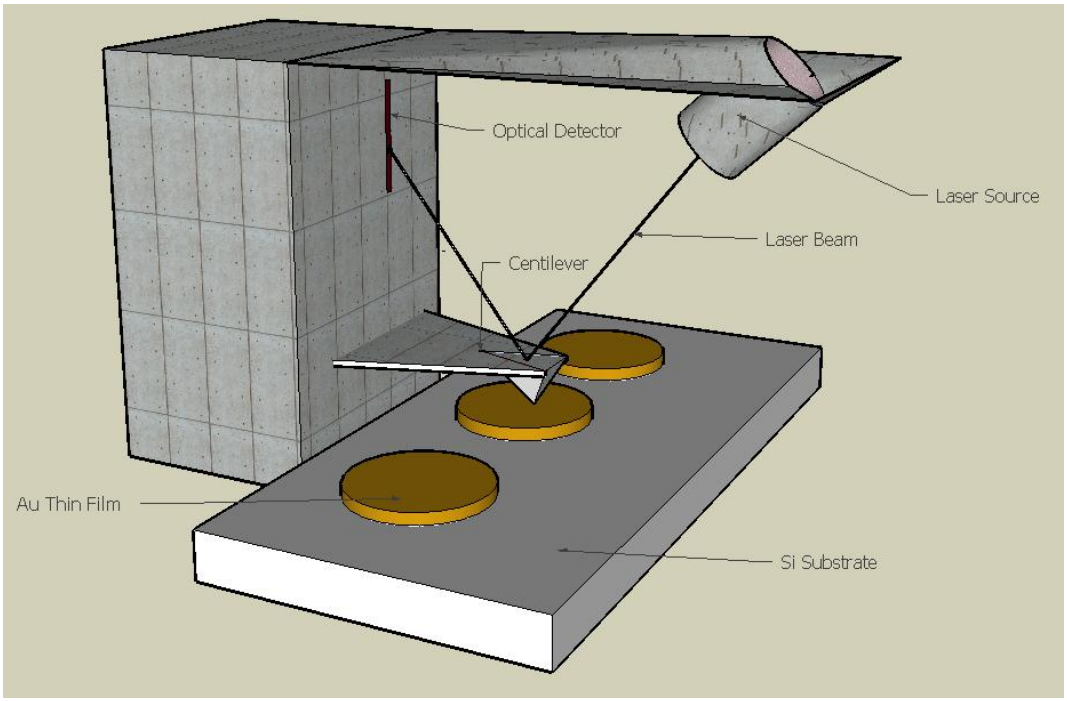

Figure 3.1 : Schematic representation of a profilometer

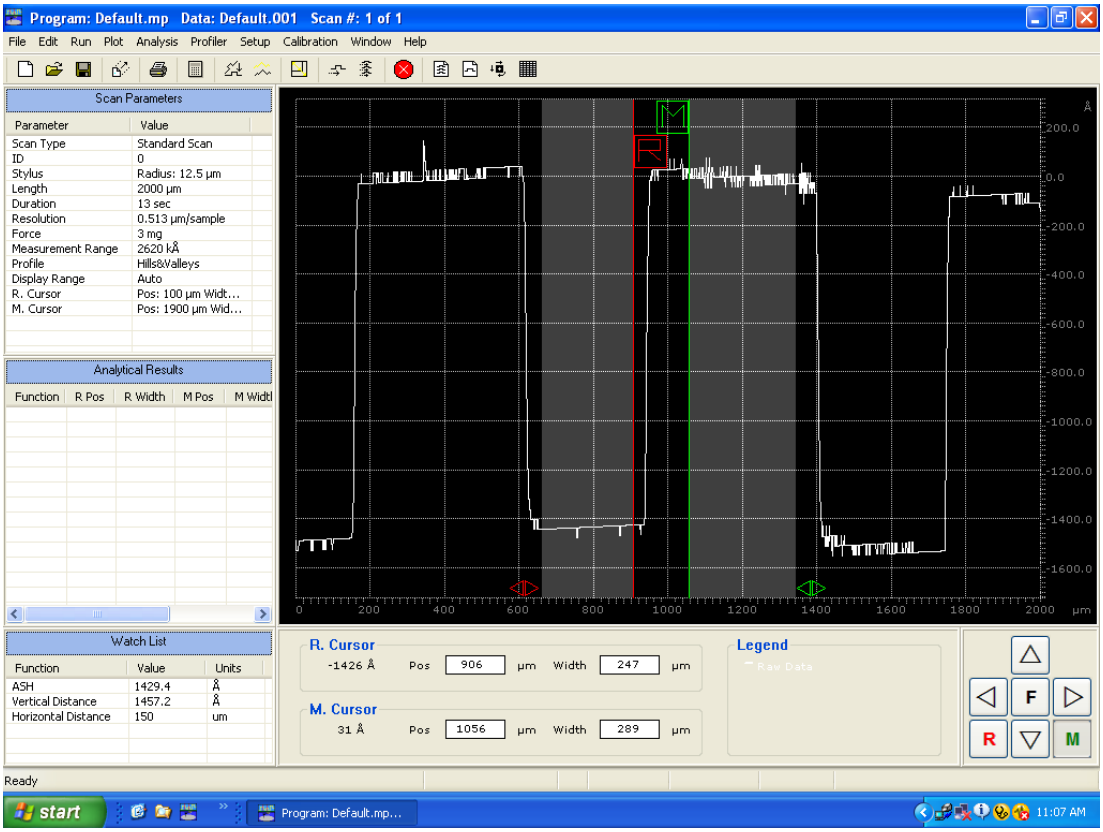

Figure 3.2 : Dektak Profilometer user interface showing average thickness of sample with steps.

Steps on the substrate are measured of and confirmed by comparing with the results of crystal thickness monitor during fabrication. In Table 3.1 the profilometer results and target thicknesses can be seen.

Table 3.1: Sample Sets Measured in Profilometer

Sample Set ID	Thickness Monitor (nm)	Profilometer(nm)
B1	25 ± 0.1	24.4 ± 0.3
B2	50 ± 0.1	51,5 ± 0.5
B3	75 ± 0.1	77.0 ± 1.1
B4	100 ± 0.1	103.3 ± 1.4
B5	125 ± 0.1	128.2 ± 1.7
B6	150 ±0.1	154.0 ± 2.2
B7	175 ± 0.1	179.4 ± 2.4
B8	200 ± 0.1	207.1 ± 2.8
C1	25 ± 0.1	24.7 ± 0.3
C2	50 ± 0.1	49.8 ± 0.6
C3	75 ± 0.1	75.1 ± 1.1
C4	100 ± 0.1	98.6 ± 1.5
C5	125 ± 0.1	127.3 ± 1.8
C6	150 ±0.1	150.4 ± 2.3
C7	175 ± 0.1	178.5 ± 2.6
C8	200 ± 0.1	205.7 ± 2.9
D1	50 ± 0.1	50.4 ± 0.6
D2	100 ± 0.1	104.4 ± 1.3
D3	150 ± 0.1	150.1 ± 2.3
D4	200 ± 0.1	200.8 ± 2.9
D5	250 ± 0.1	248.9 ± 3.5
D6	300 ±0.1	300.3 ± 4.2
D7	350 ± 0.1	347.7 ± 4.8
D8	400 ± 0.1	396.7 ± 5.3

3.2 Ellipsometer Measurements

The thicknesses of optically transparent coatings are generally measured by an optical method: Ellipsometer. The precision of the method is very high (up to 1 or 2 nm) if the thickness range of the film is predefined. In the present study, ellipsometer is used for measuring thickness of silicon dioxide thin films on silicon substrate. Silicon dioxide is optically transparent to visible range and the system is using 650 nm wavelength LASER so that it is transparent. The measurement range of the system is from 2-3 nm to microns.

On the other hand, thickness measurements of gold, germanium and aluminum films are impossible because of opacity of these materials to visible 650nm wavelength. The ellipsometer system used in this study can be seen in Figure 3.3.

Figure 3.3: Ellipsometer used in my experiments for silicon dioxide thin film thickness measurements. LASER source is located on the left side. The samples are put on the stage in the middle and the detector is on the right side.

The results of ellipsometer measurements can be seen in Table 3.2. The predicted thickness and measured thickness in ellipsometer for silicon dioxide samples are close to each other.

Table 3.2: Sample Sets Measured in Ellipsometer

Sample Set ID	Calculated Thickness(nm)	Ellipsometer Measurement(nm)
E1	50 ± 5	55 ± 0.3
E2	100 ± 10	101 ± 0.6
E3	150 ± 15	155 ± 0.9
E4	200 ± 20	210 ± 1.2
E5	250 ± 25	244 ± 1.5
E6	300 ±25	297 ± 1.8
E7	350 ± 25	355 ± 2.2
E8	400 ± 25	418 ± 2.5

3.3 SEM Cross-sectional Thickness Imaging

For verification of the film thicknesses, samples are analyzed by a scanning electron microscope. Specimens are prepared cross-sectional and thin film thicknesses are measured by microscope's software. In the Figure 3.4, SEM images of gold samples and the film thickness measured by imaging software can be seen.

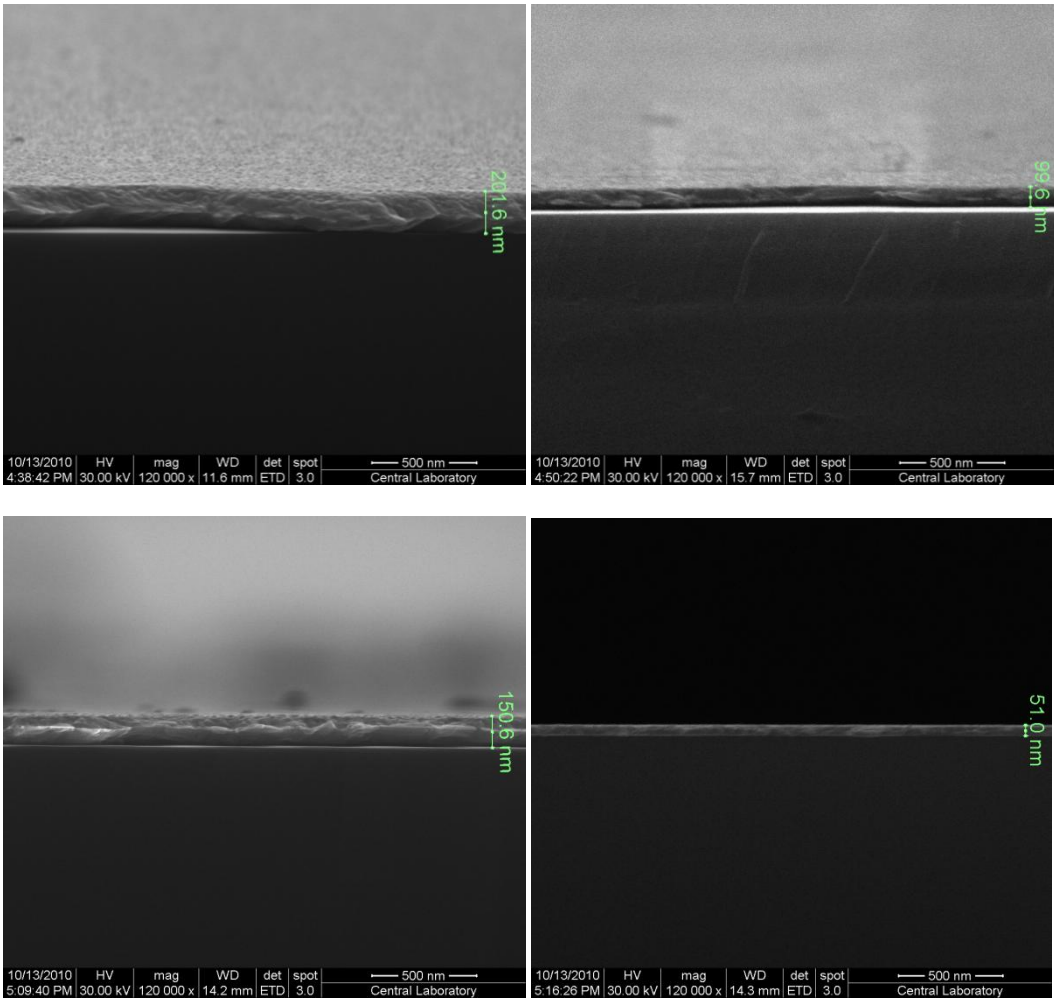

Figure 3.4: Cross-Sectional SEM images of gold thin film samples at different thicknesses a- 50 nm b- 100 nm c- 150 nm d- 200 nm.

3.4 EDS Measurements

Energy dispersive x-ray spectrometer system that is used in this study is a EDAX brand with lithium doped silicon detector which is cooled by liquid nitrogen.

Energy dispersive x-ray spectrum measurements are done on each sample with different accelerating voltages. For each voltage, the amplification time of the detector is tuned for optimum dead time (around %30). For that reason, smaller spot sizes and smaller amp times are used for higher voltages, and larger spot sizes and larger amp times for lower voltages. Amp times and spot sizes used in the experiments can be seen in Table 3.3.

Table 3.3: Amp time and spot size for different acceleration voltage of electrons in EDS measurements

Energy of Electrons (keV)	Amp Time (μs)	Spot Size (in arb. u.)
30	12,8	5
29	12,8	5
28	12,8	5
27	12,8	5
26	12,8	5
25	12,8	5
24	25,6	5
23	25,6	5
22	25,6	5
21	25,6	5
20	25,6	5
19	25,6	5
18	25,6	5
17	25,6	5
16	25,6	5
15	25,6	5
14	51,2	5
13	51,2	5
12	102,4	5
11	102,4	5
10	102,4	5
9	102,4	6
8	102,4	6
7	102,4	7
6	102,4	7
5	102,4	7
4	102,4	7
3	102,4	7

During the fabrication process of metallic coatings a mask is used for creating steps on the surface to be able to measure them in profilometer. The diameter of the steps is around 400 microns and the edge of the rectangle where EDS data is collected from is 50-60 microns at the center of the 100 micron diameter dot. The dot and the rectangle EDS data comes from can be seen in Figure 3.5.

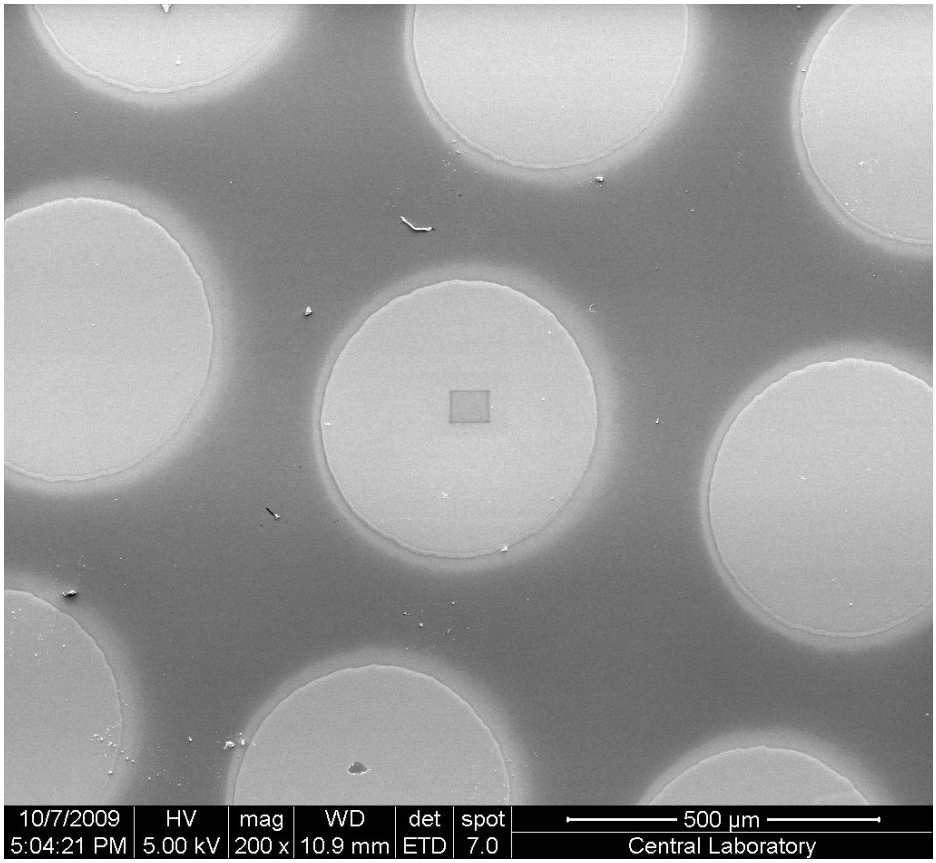

Figure 3.5: SEM image of the steps showing the gold dots created during fabrication the zone EDS data collected from.

EDS spectrum includes peaks from the elements' relaxation energies. For higher atomic number elements K transition energies are very high to observe so that, for higher atomic number elements, L and M transitions are observed in EDS spectrum. In Figure 3.6, EDS spectrum and data output of EDS system of germanium thin film on silicon substrate can be seen. Electron energy for this measurement is 23 keV and total spectrum collection time (Lsec) is 10 seconds. Silicon K transition and germanium L transition peaks can easily be seen in the figure. Moreover, EDS system gives ZAF correction coefficients for the measurement. After ZAF corrections, atomic ratios of germanium and silicon are used further calculations.

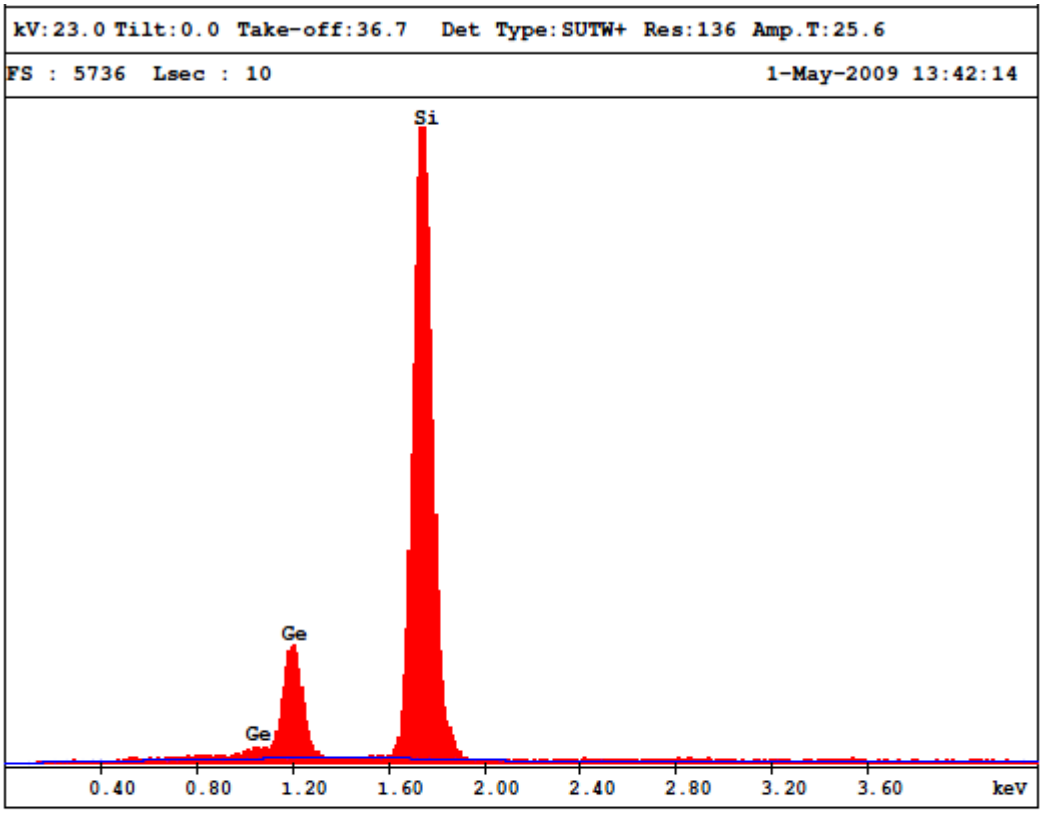

EDAX ZAF Quantification (Standardless)
Element Normalized
SEC Table : Default

Element	Wt %	At %	K-Ratio	Z	A	F
GeL	20.27	8.96	0.1977	0.8685	1.1070	1.0144
SiK	79.73	91.04	0.5355	1.0294	0.6525	1.0000
Total	100.00	100.00				

Element	Net Inte.	Bkgd Inte.	Inte. Error	P/B
GeL	694.90	40.83	1.25	17.02
SiK	4203.27	38.87	0.49	108.13

Figure 3.6: EDS Spectrum and Elemental Ratio output of EDS system for Ge sample.

CHAPTER 4

SIMULATION AND THICKNESS DETERMINATION

4.1 EDS Atomic Ratio(EAR) and Thickness Relation

The EDS data output of EDS system is just atomic ratios of the elements. For a specific thin film on a substrate, the system gives only the elemental ratio of coating element and the substrate. The interaction volume of the electrons increases with the energy of the electron so that, by increasing the energy of the electrons, it is possible to increase the interaction volume resulting, deeper data collection. Deeper data collection means that electrons can reach substrate and x-rays from the substrate can be observed [26]. For a constant electron energy, for different thicknesses of thin films, EDS gives different ratios. From this point of view, for different thicknesses of films, by using different energies of electrons, EDS Atomic Ratio & Electron Energy graphs of thin films can be constructed. In this study gold, aluminum, germanium and silicon dioxide thin films at different thicknesses are analyzed for constructing EDS Atomic Ratio & Electron Energy graphs.

First sample set of the experiments is gold thin films from 25nm to 200 nm. Gold is a very dense material and electron interaction volume is very low compared with other lighter materials. In the Figure 4.1 it is seen that, EDS gold ratio decrease with electron energy increase. Moreover, the shift in the graph for different thicknesses can be seen in the figure. The curves shift to the right with

higher thickness of the film. The raw data for gold film can be found in Appendix B.

As can be seen from this graph the thickness of an unknown gold film on Si substrate can easily be determined if the data presented in Figure 4.1 can be stored in some data base and then recalled during the measurement.

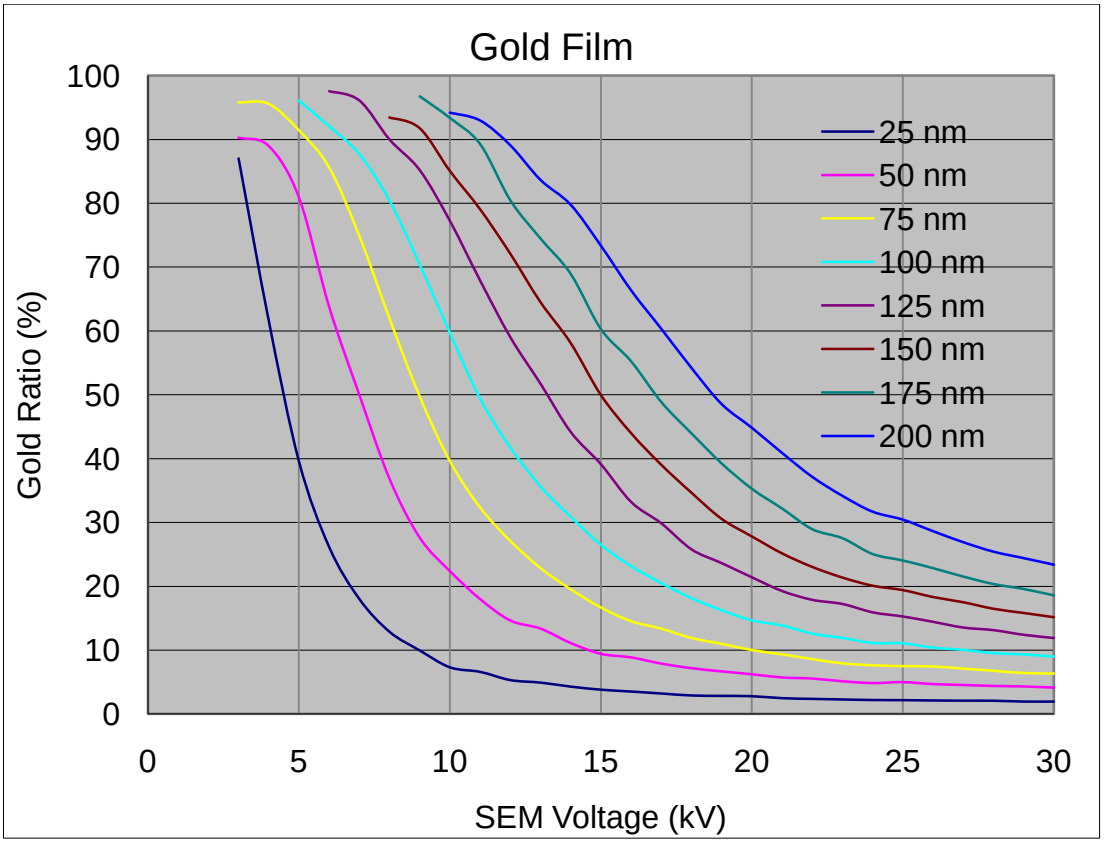

Figure 4.1: SEM Voltage & Gold Ratio Graph for different thickness gold films on Si substrate.

Second set of the experiments include germanium thin films on silicon substrate. The thicknesses of the samples are same as gold ones: 25nm to 200 nm. In the figure 4.2, it is seen that EDS germanium ratio decreases as the electron energy increase. Moreover, for higher thicknesses, there is a right shift in the graph but the shift rate is not as much as shift rate in gold. The reason for this result is the density difference of the materials. The raw data for germanium film can be found in Appendix C.

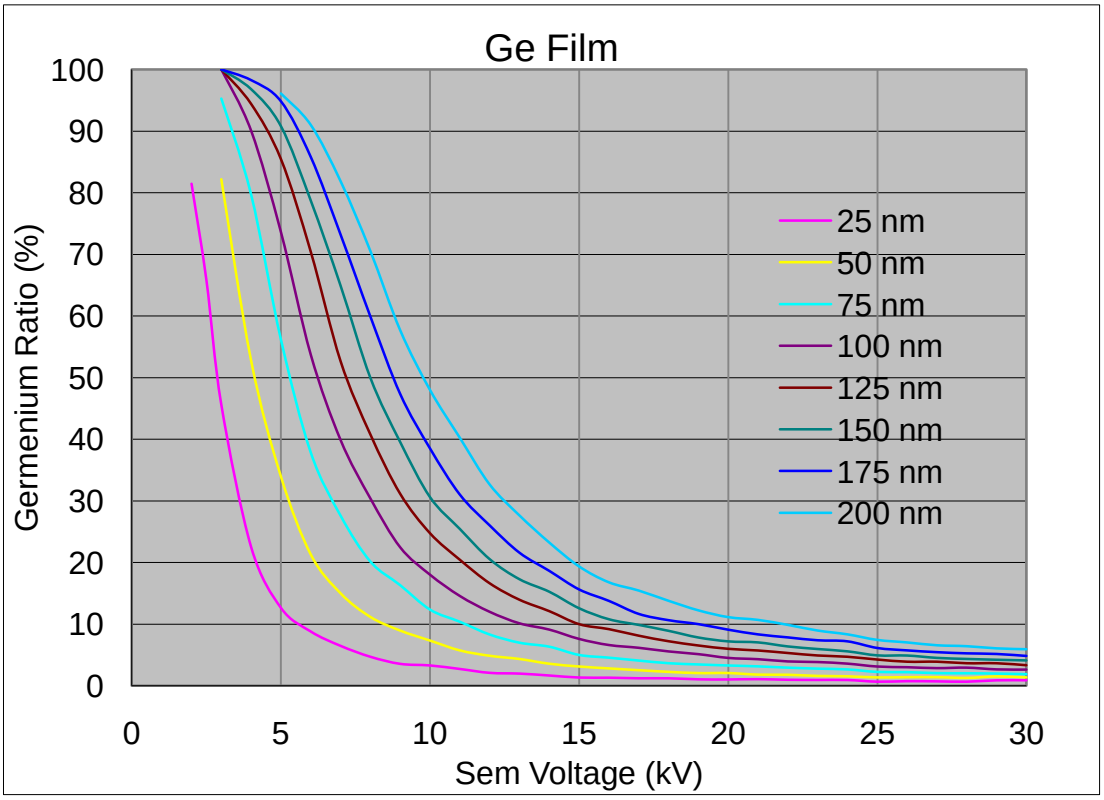

Figure 4.2: SEM Voltage & Germanium Ratio Graph of different thickness germanium films on Si substrate.

Another sample set is aluminum on silicon substrate. The density of aluminum is so low that the thickness for this set is enlarged from 25nm - 200 nm to 50 nm - 400 nm. Similar to previous sample sets, EDS aluminum ratio decrease with electron energy as can be seen in Figure 4.3. The right shift of the curve for different thicknesses is also observed. The shift rate is smaller than the germanium samples because the density of aluminum is smaller than germanium. The raw data for aluminum film can be found in Appendix D.

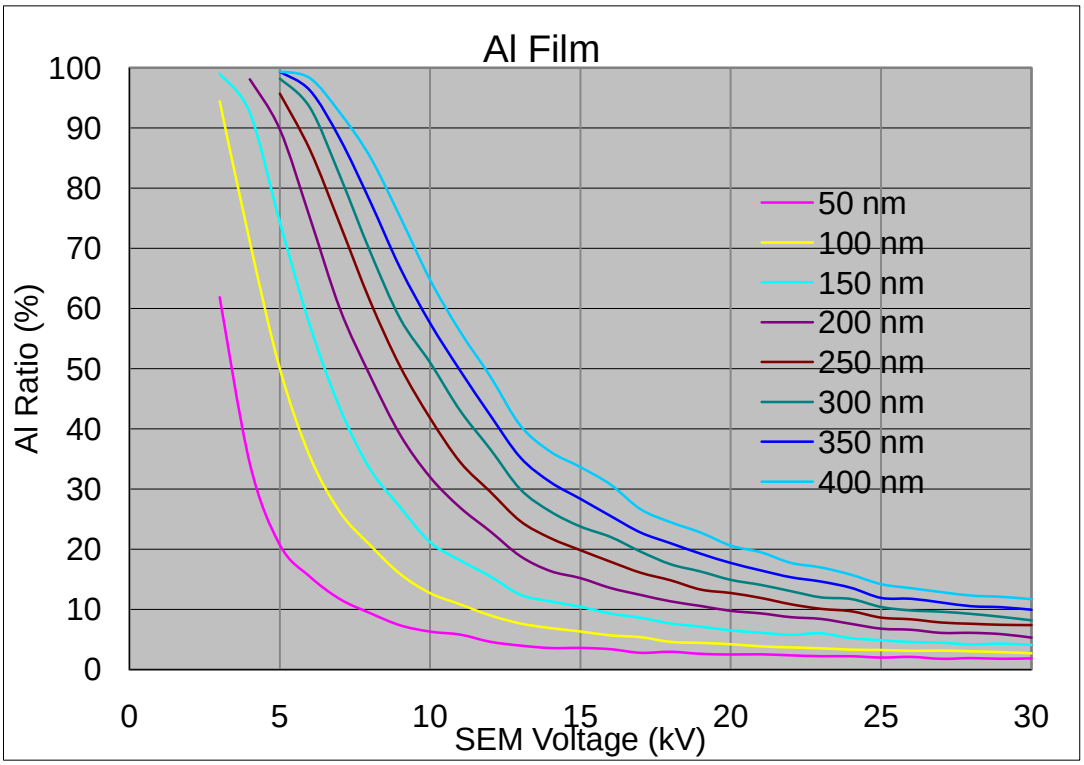

Figure 4.3: SEM Voltage & Aluminum Ratio Graph of different thickness aluminum films on Si substrate.

After analyzing pure elemental materials as a coating, a simple compound silicon dioxide thin film on silicon substrate is analyzed. In Figure 4.4, similar curves for different thicknesses can be seen. Different from previous samples, oxygen ratio converges to 66% on the left side of the graph because of the stoichiometric ratio of oxygen in silicon dioxide. The raw data for silicon dioxide film can be found in Appendix E.

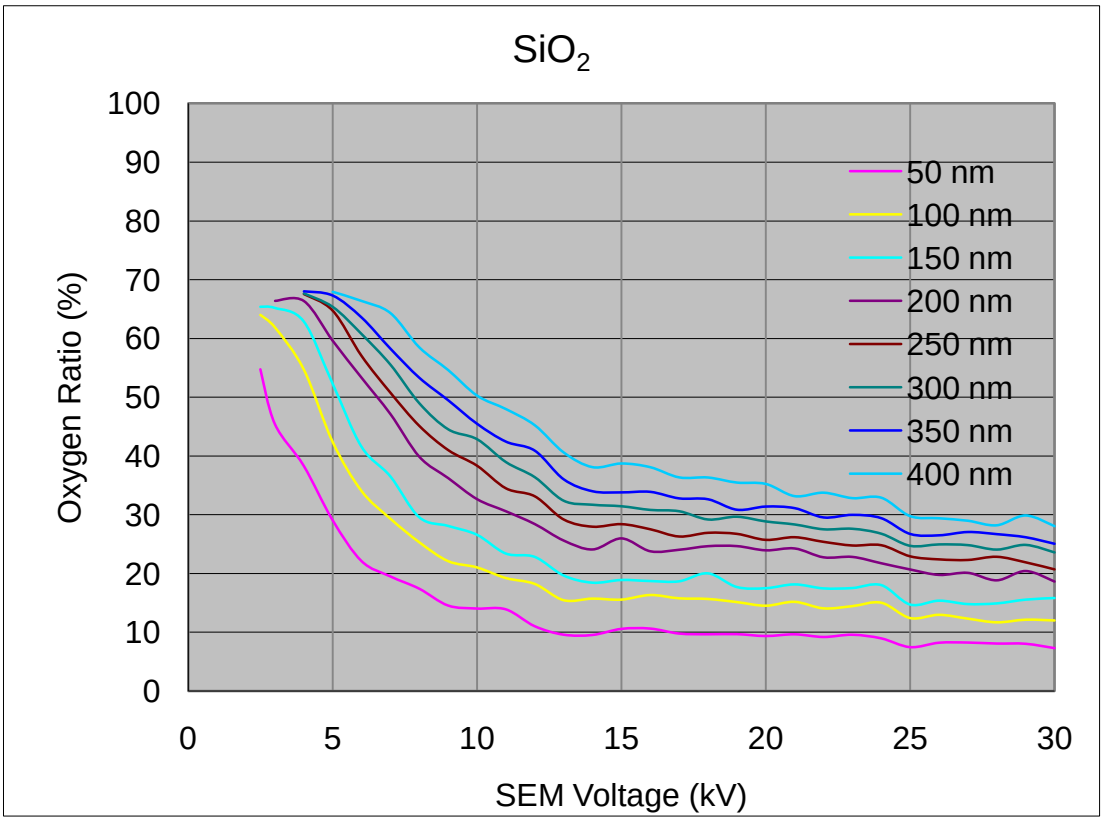

Figure 4.4 : SEM Voltage & Oxygen Ratio Graph of different thickness silicon dioxide films on Si substrate.

4.2 Electron Beam Simulator (CASINO)

The reference data does not need to be constructed just with using data obtained from reference samples. We can also construct reference data by a simulation. CASINO (monte **Ca**rlo **Si**mulation of electro**n** Trajectory in S**o**lids) is a simulation software running on windows operating system, which can simulate electrons, and emitted x-rays coming from the solids and we can construct the reference data by using CASINO [27]. CASINO is free software available on internet [28].

First of all, the substrate must be determined in the simulation. Then the films on the substrate with the specific thickness should be constructed. After defining the sample, simulation parameters of electrons must be set. It is an option that multiple energies of electrons can be simulated in one simulation run. Once the number of electrons to simulate is set and the simulation can be started.

The result of the simulation gives us electron trajectories deep inside the sample. Interaction volume of electrons in the sample can be easily seen on the graphical interface. Moreover, the software gives us the number of generated x-rays for each electron for a specific thickness for each electron energies. By using these numbers, elemental ratio of the thin film which is expected from EDS result can be calculated. In the Figure 4.5, Monte Carlo Simulation of 100 nm aluminum thin film on silicon substrate at 10keV can be seen.

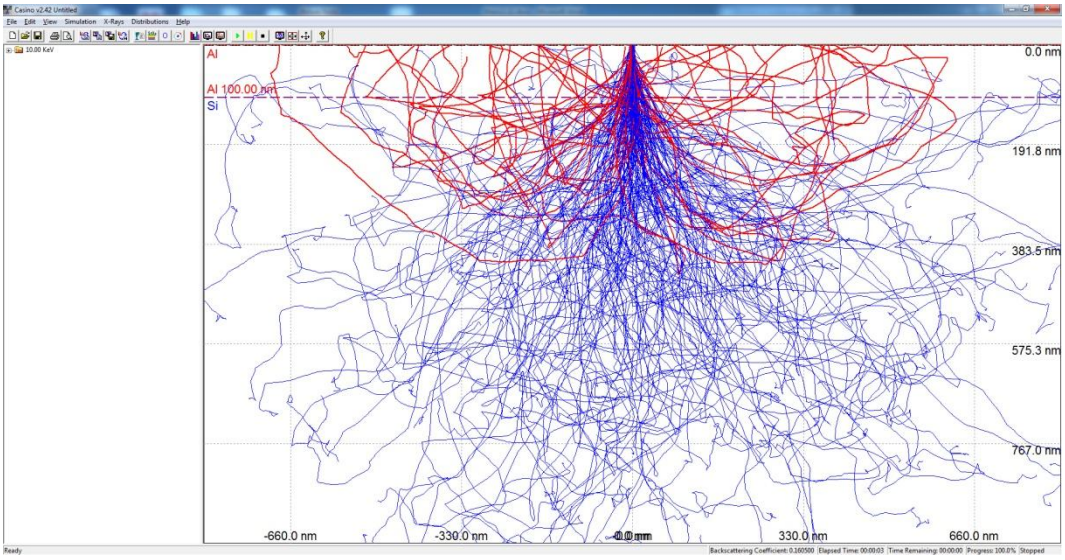

Figure 4.5 : Monte Carlo Simulation of 100 nm aluminum thin film on silicon substrate at 10keV.

The ratio results are used for constructing the Voltage-Elemental Ratio graph and in Figure 4.6 it is seen that the graph is similar to experimental result which is given before in Figure 4.1.

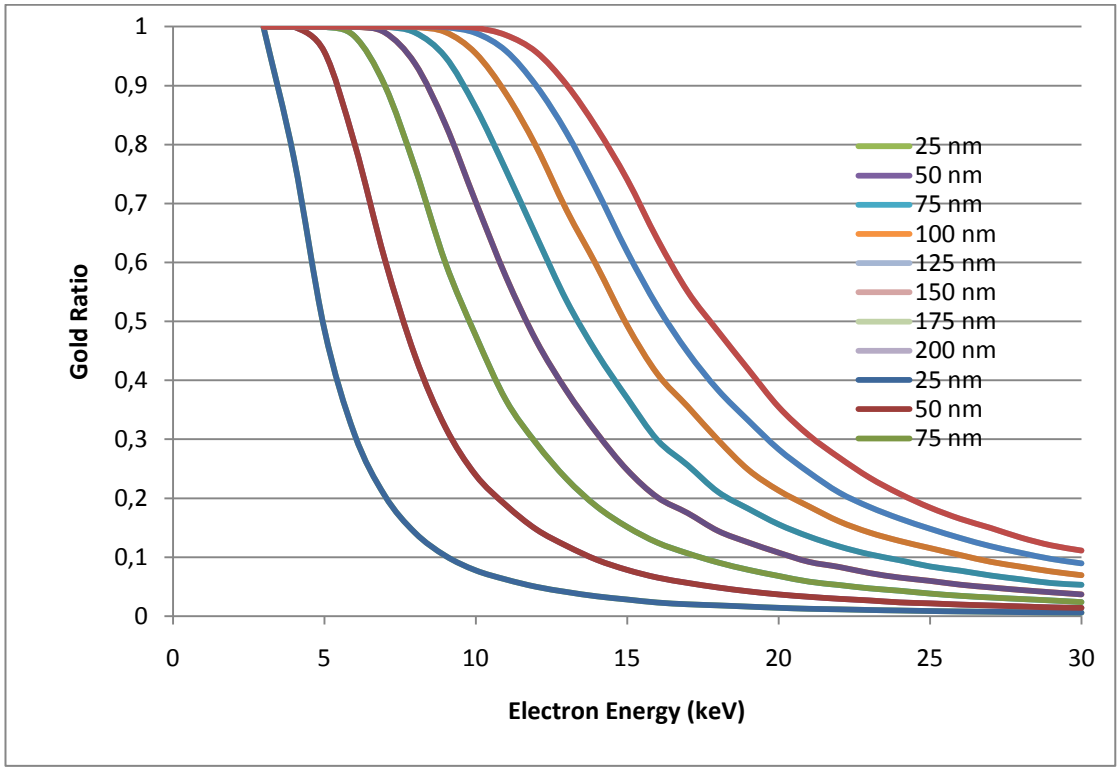

Figure 4.6 : Monte Carlo simulation of Voltage & Gold Ratio Graph for different thickness gold films on Si substrate.

4.3 Interaction Volumes of Film and Substrate

The interaction volume of electrons can be simply considered as a sphere and volume percentage of the thin film and the substrate can be calculated by the formulas:

$$V_f = \pi . (h^2.r - h^3/3) \quad (3)$$

and

$$V_s = 4/3 . \pi . r^3 \quad (4)$$

The volumes can be seen in Figure 4.7.

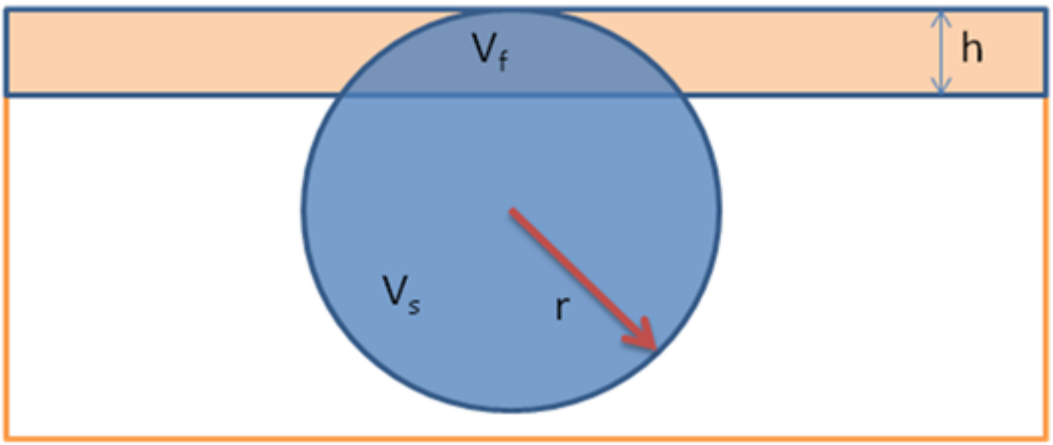

Figure 4.7: Sphare representing electron interaction volume on the sample.

By increasing the sphere radius for the same film thickness. Figure 6.1 can be obtained. The shape of the curve in the Figure 6.1 is similar to experimental results and simulation results.

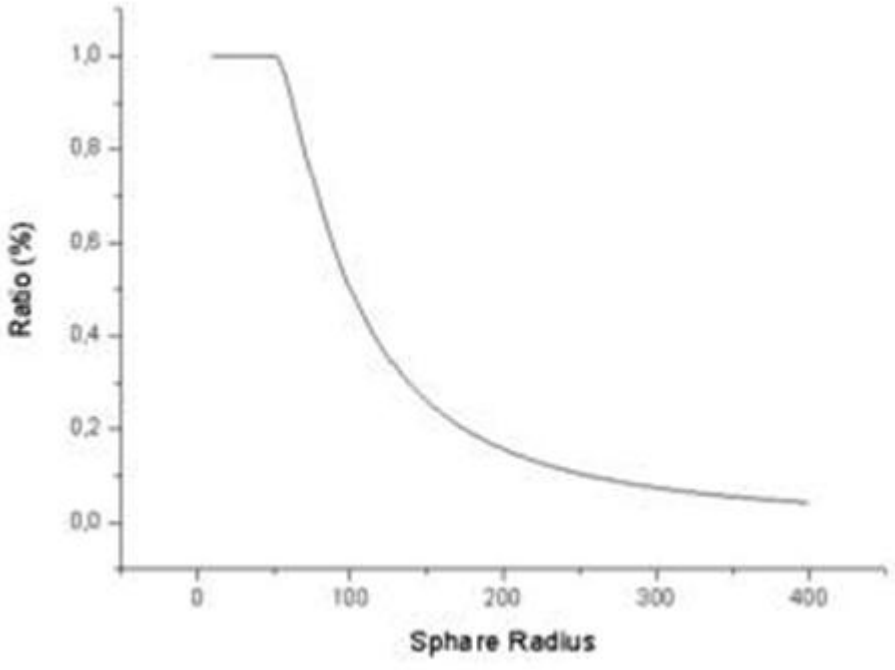

Figure 4.8: Sphare Radius & Thin Film ratio calculation from the formulas.

4.4 Thickness Determination Software

The thickness determination method can be faster by a software which automatically collects EDS data from EDS software and calculates the thickness. For that reason, a software is developed on LABVIEW platform, which is suitable for constructing laboratory based programs for data collecting and data processing in a graphical interface. LABVIEW platform is also suitable for connecting other hardware system by several network protocols such as USB or Ethernet so it is possible that, in the future, the software can be directly linked to EDS hardware and the data is directly collected in by the SEM-EDS system.

The software that we developed, first requests EDS data from EDS hardware by sending EDS parameters such as electron energy in keV, spot size of the electron beam, dwell time and live time for data collection. When EDS analysis finishes for a specific electron energy, it gets elemental ratios of the substrate and the film for that electron energy. It repeats the data collection for different electron energies 3keV to 30keV with steps of 1keV. After collecting elemental ratios for each electron energies, the software constructs a table of elemental ratios versus electron energy. The software interface can be seen in Figure 4.9.

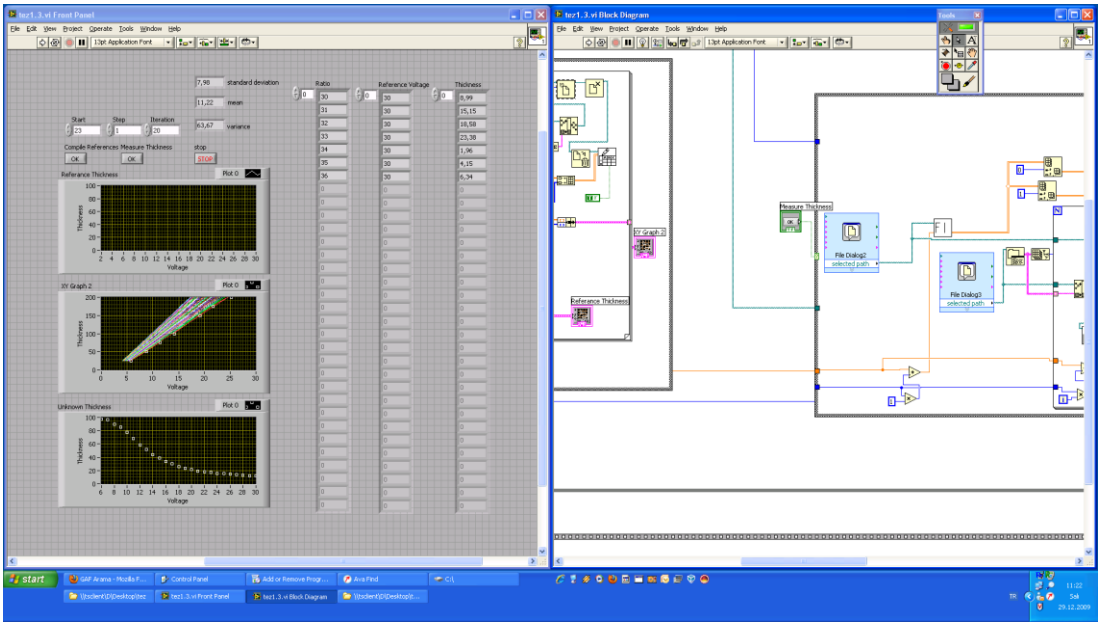

Figure 4.9: Thickness determination software constructed in LabView.

The software also gets elemental data for substrate and film from the EDS system. For that specific substrate and the film, the software checks its library for a reference data. If there is a reference data created before for that specific substrate and film, the software uses that data. If there is not such reference data, the software tries to connect to electron simulator for first time creation of the reference data. After creation of reference data, the software has both all reference data and unknown film's data.

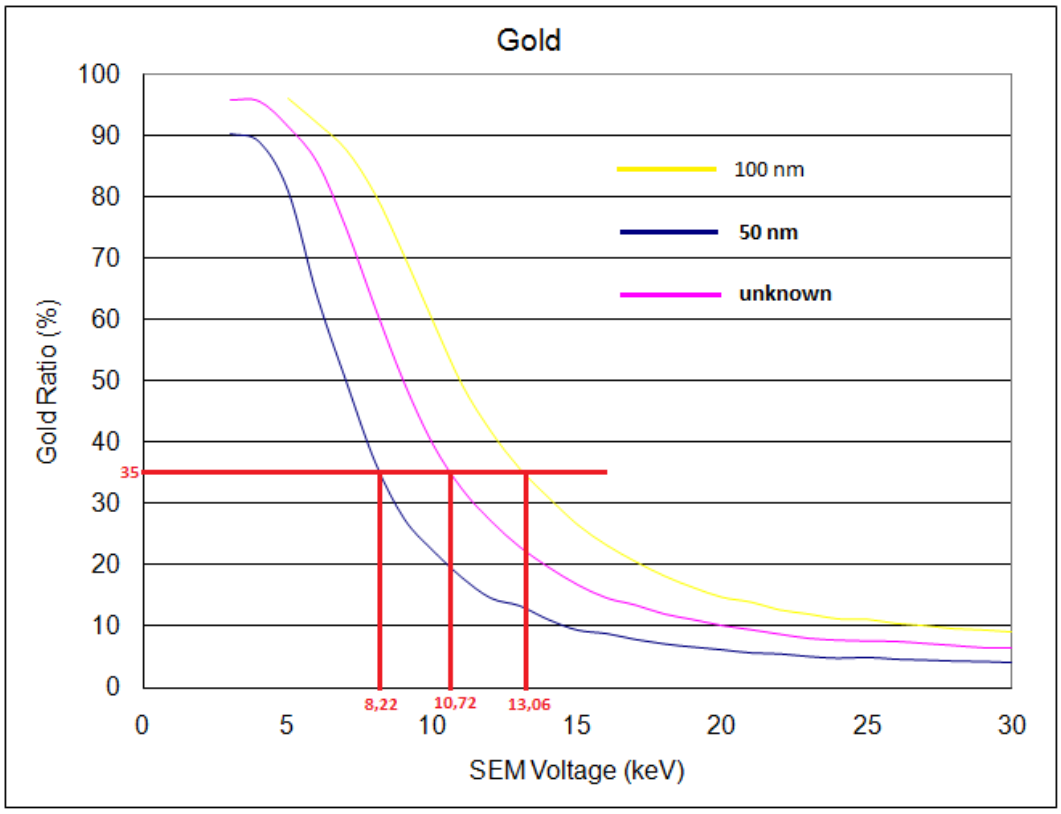

Figure 4.10 Interpolation of unknown sample's curve for a specific EDS ratio of 35 % gold.

At this stage, the software draws a horizontal line on the graph for a specific elemental ratio (for example %35). Then it interpolates the curves of reference and unknown films. It determines the intersection of the horizontal line and unknown film's curve. The software obtains the energy value of intersection point. Furthermore, the software determines the intersection of neighboring reference curves of unknown's curve and similarly it obtains the energy values for their intersection points which can be seen in Figure 4.10. Now, the software has the energy values of unknown sample and two neighboring reference data for a specific elemental ratio(for example %30). By linearly interpolating two neighboring reference data, the software can easily determine the unknown sample's thickness which can be seen in Figure 4.11. Moreover, the software

repeats these steps for different elemental ratios from a range of 30% to 70% with steps 1% and, for each elemental ratio, the thickness is determined.

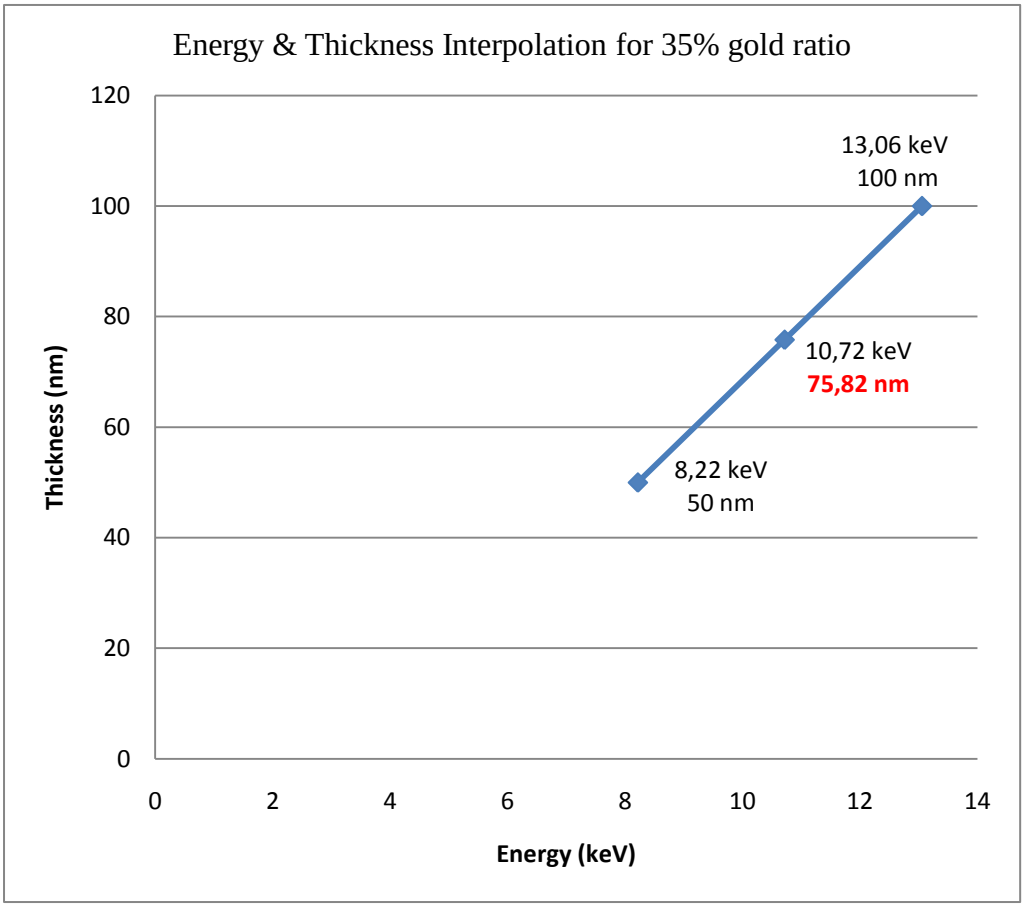

Figure 4.11: Linear interpolation of unknown film with known (50 nm and 100 nm) films.

In Table 4.1, gold samples thickness determination results can be seen. These results are obtained by considering the specific thickness is unknown, and others are known and used as reference data. For that reason, the software can not produce any result for 25 nm and 200 nm samples because there is not enough reference data for these samples.

Table 4.1: Determined thicknesses by the software comparison chart to measured thicknesses of gold samples.

Thickness Determined from EDS measurements (nm)	Thickness measured from Thickness Monitor (nm)	Thickness Determined from Profilometer (nm)
-	25 ± 0.1	24.4 ± 0.3
48.9 ± 0.6	50 ± 0.1	51.5 ± 0.5
75.3 ± 0.8	75 ± 0.1	77.0 ± 1.1
102.4 ± 2.2	100 ± 0.1	103.3 ± 1.4
127.5 ± 2.3	125 ± 0.1	128.2 ± 1.7
155.2 ± 2.4	150 ±0.1	154.0 ± 2.2
177.1 ± 1.9	175 ± 0.1	179.4 ± 2.4
-	200 ± 0.1	207.1 ± 2.8

In Table 4.2, germanium samples' thickness determination results can be seen. Similarly, these results are obtained from the developed software. The standard deviation of determined thickness of germanium samples are higher than gold because of the resolution of the thickness determination method, we developed.

Table 4.2: Determined thicknesses by the software comparison chart to measured thicknesses of germanium samples.

Thickness Determined from EDS measurements (nm)	Thickness measured from Thickness Monitor (nm)	Thickness Determined from Profilometer (nm)
-	25 ± 0.1	24.7 ± 0.3
52.1 ± 0.9	50 ± 0.1	49.8 ± 0.6
73.3 ± 1.2	75 ± 0.1	75.1 ± 1.1
100.7 ± 2.8	100 ± 0.1	98.6 ± 1.5
128.5 ± 2.5	125 ± 0.1	127.3 ± 1.8
150.2 ± 2.9	150 ±0.1	150.4 ± 2.3
177.2 ± 2.6	175 ± 0.1	178.5 ± 2.6
-	200 ± 0.1	205.7 ± 2.9

In Table 4.3, aluminum samples' results can be seen. Determined thicknesses of aluminum samples are in tune with thickness monitor and profilometer measurements.

Table 4.3: Determined thicknesses by the software comparison chart to measured thicknesses of aluminum samples.

Thickness Determined from EDS measurements (nm)	Thickness measured from Thickness Monitor (nm)	Thickness Determined from Profilometer (nm)
-	50 ± 0.1	50.4 ± 0.6
102.1 ± 0.6	100 ± 0.1	104.4 ± 1.3
147,8 ± 1.8	150 ± 0.1	150.1 ± 2.3
199,7 ± 2.8	200 ± 0.1	200.8 ± 2.9
253,9 ± 3.3	250 ± 0.1	248.9 ± 3.5
299,6 ± 4.8	300 ±0.1	300.3 ± 4.2
354,3 ± 4.2	350 ± 0.1	347.7 ± 4.8
-	400 ± 0.1	396.7± 5.3

In table 4.4, silicon dioxide samples' results can be found. Silicon dioxide films' thicknesses standard deviations are higher than elemental films thicknesses. The reason is the complexity of the compound.

Table 4.4: Determined thicknesses by the software comparison chart to measured thicknesses of silicon dioxide samples.

Thickness Determined from EDS measurements (nm)	Thickness from oxidation chart during fabrication (nm)	Ellipsometer (nm)
-	25 ± 5	55 ± 0.3
105.9 ± 3.6	50 ± 10	101 ± 0.6
155.3 ± 3.8	75 ± 15	155 ± 0.9
203.0 ± 2.9	100 ± 20	210 ± 1.2
248.1 ± 4.3	125 ± 25	244 ± 1.5
299.2 ± 5.4	150 ± 25	297 ± 1.8
347.1 ± 5.9	175 ± 25	355 ± 2.2
-	200 ± 25	418 ± 2.5

CHAPTER 5

CONCLUSION

Both in the industrial and research-development application, the thickness measurement of thin films has become increasingly important in recent years. There are various methods for thickness measurement but nearly all of them have disadvantages or limitations. In this thesis, a the method of thickness determination by a EDS based technique has been studied. In this method, an EDS system in which electron-matter interaction is utilized to generate and measure x-rays, is used to determine the thickness of a thin film deposited on a substrate. EDS is usually attached to a scanning electron microscope (SEM) system with imaging capability. . The data obtained from EDS is compiled and used for constructing a reference table for the specific substrate and element. Then the reference data is used for determining the thickness of the unknown sample by analyzing and constructing the data. Moreover, the reference data can be easily constructed by a monte carlo simulation in cases where no previously measured and stored data are available. So it is not always necessary to have reference samples for thickness determination process. SEM is a widely used and practical tool in material science and nanotechnology and most of the laboratories in research and development area possesses a SEM system. As is known, EDS systems are also very commonly attached to SEMs and frequently used. From this point of view, the thickness determination method can be applied to any kind of SEMs attached with EDS system just by a software installation. It will bring a new capability this system. Moreover the method has some advantages compared to other thickness measuring techniques. It is a nondestructive method and the electron beam spot where the thickness can be measured, can be selected just by

using SEM's image. Furthermore, this feature makes it possible to map the thickness variations over large surfaces. Vacuum compatibility is the only condition for the specimen and nearly every elemental coating can be examined by this method. For compounds, the system works again but there is an uncertainty in the measured thickness. The uncertainty increases with the complexity of composition of the compound. However, in this study it is shown that, some simple compounds' thickness can also be measured by the method. The standard deviations of the thickness for compounds are higher than elements.

The thickness determination range varies with the density of the coating. In denser materials, electron mean free path is lower compared with lighter materials. The interaction volume of the electron decreases with higher density resulting in that electrons can not reach deeper inside the coating. For that reason high density coatings such as gold, the thickness measuring limit is 1 micron even 30keV is used. For thicker samples, the technique is useless. For low density materials like aluminum, larger interaction volume enables thicker measuring limit which is nearly 2,5 microns for aluminum.

The fabrication method of my study differs compared to referred studies. In F.L Ng's and Zhuang's study, magnetron sputtering, in Möller's study, electron beam PVD is used. On the other hand, characterization of the samples are all done by profilometer. Additionally, TEM imaging is used in Sempf's study. Instead of TEM, SEM imaging is used in this work. In this thesis as thin film, Ge and silicon dioxide are used, which are not analyzed before. Au and Al thin films are also analyzed and results are compared with similar studies in literature. In this study, the difference of the thicknesses from profilometer and from the calculated results is below %3, which is 10% in Zhuang's study.

Comparison of the thesis and literature can be seen in Figure 5.1. Compared to similar studies in the literature, the results are consistent to each other and a direct

method is given in this study. By using this direct method, a new software, which can be similar to ThinFilmID but open source one, can be developed.

Table 5.1: Comparison of the thesis and the literature.

	Thesis	**Literature**
Sample Preperation	Thermal Evoporation Wet Oxidation	PVD (e-beam melting) Magnetron Sputtering Spin Coating
Results Verification	Oscillating quartz Profilometer Ellipsometer SEM Imaging Simulations	SIMS , RBS (Möller et al) Oscillating quartz Profilometer, Simulations, SEM Imaging Ellipsometer
Films & Substrate	Au, Al, Ge SiO_2 films on Si substrate from 50nm to 400nm	Cu (Möller et al) FeCoSiB (Zhuang et al) Al,Ni,Au (Ng et al) TiO_2, ZrO_2 (Sempf et al) On Si substrate
Results	Atomic Ratio is used	K-ratio is used (Möller et al) Intensity ratio and Sewel formula is used (Zhuang et al) Critical Voltage is defined(Ng et al)
Thickness Calculation	A general method is introduced. Explained A software princible is introduced.	No any general method. Just specific films are discussed. ThinFilmID is used but it is a commmercial software.

As a future work, multi layer thin films can be studied. In multilayer structure, EDS elemental ratios can be analyzed for varying electron energies. The software can be modified and developed for accurate results for multi layer structures.

REFERENCES

[1] K. L. Chopra1, P. D. Paulson and V. Dutta1, Thin-Film Solar Cells: An Overview, Prog. Photovolt: Res. Appl. 2004; 12:69–92 (DOI: 10.1002/pip.541)

[2] Ferroelectric thin films for micro-sensors and actuators: a review P Muralt Ceramics Laboratory, Materials Department, EPFL Swiss Federal Institute of Technology, CH-1015 Lausanne, Switzerland

[3] Direct and inverse measurement of thin films magnetostriction Jay, J.-Ph., Le Berre, F., Pogossian, S.P., Indenbom, M.V. 2010 Journal of Magnetism and Magnetic Materials 322 (15), pp. 2203-2214

[4] Influences of thickness-uniformity and surface morphology on the electrical and optical properties of sputtered CdTe thin films for large-area II-VI semiconductor heterostructured solar cells Choi, Y.-O., Kim, N.-H., Park, J.-S., Lee, W.-S. 2010 Materials Science and Engineering B: Solid-State Materials for Advanced Technology 171 (1-3), pp. 73-78

[5] ZnO-based transparent thin-film transistors Hoffman, R.L., Norris, B.J., Wager, J.F. 2003 Applied Physics Letters 82 (5), pp. 733-735

[6] Metal Oxide Semiconductor, http://en.wikipedia.org/wiki/Metal_Oxide_Semiconductor#Metal.E2.80.93oxide.E2.80.93semiconductor_structure, last accessed date: 13/09/2010

[7] Thin film studies using multiple-beam interferometry, J. N. Israelachvili Journal of Colloid and Interface Science Volume 44, Issue 2, August 1973, Pages 259-272

[8] New Hampshire Materials Laboratory, Scanning Electron Microscopes, http://www.nhml.com/resources/1998/10/1/scanning-electron-microscopes-sem, last accessed date: 09/13/2010

[9] Maurizio Dapor (2003), Electron Beam Interactions with Solids, Springer, Verlac, Berlin

[10] Özenbaş M. (2007) Scanning Electron Microscopy, Introduction to Micro and Nanotechnology 502, Lecture Notes, p 17,22.

[11] Harry Verhulst (2008) EDAX Genesis EDS Short Course Lecture Notes, EDAX, The Netherlands

[12] Goldstein, J. I.; Newbury, D. E.; Echlin, P.; Joy, D. C.; Lyman, C. E.; Lifshin, E.; Sawyer, L. C.; Michael, J. R. (2003), Scanning Electron Microscopy and X-Ray Microanalysis, Springer, ISBN 0306472929, p 84,240,294,295.

[13] Micron Inc. Analytical Service Laboratory, http://www.micronanalytical.com/sem.html, last accessed date: 13/09/2010

[14] V.H. Heywood (1971), Scanning Electron Microscopy , Academic Press, London, Newyork

[15] X-ray Data Booklet, Low Energy Electron Ranges in Matter, http://xdb.lbl.gov/Section3/Sec_3-2.html, last accessed date: 13/09/2010

[16] Reed, B. Electron Microprobe Analysis, 2nd Ed., Cambridge University Press, Cambridge, 1993, p 240.

[17] Pouchou J.L., Pichoir F. Rech. Aerosp. 1984,3,13-1984,4,47.

[18] Pouchou J.L., Pichoir F.,Electron Probe Quantitation, Plenum, New York, 1991, p31.

[19] Möller A, Weinbruch S., Stadermann F.J., Ortner H.M., Neubeck K., Balogh A.G., Hahn H., Accuracy of Film Thickness Determination in Electron Probe Microanalysis, Mikrochimica Acta 119, 1995, p 42,43.

[20] Zhuang L., Bao S., Wang R., Li S., Ma L., Lv D., ,IEEE Proceedings of Applied Superconductivity and Electromagnetic Devices, 25-27 Sept. 2009, p 142,143.

[21] Ng F.L., Wei J., Lai F.K., Goh K.L., Thickness measurement of metallic thin film by X-ray microanalysis, SIMTech Technical Reports, Vol 10, Nbr 1 Jan-Mar 2009, p 21,23,25.

[22] ThinFilmID, Oxford Instruments, http://www.oxinst.com/products/microanalysis/eds/eds-software/thin-film-inspection/Pages/thinfilmid.aspx, last accessed date: 13/09/2010.

[23] Sempf K., Herrmann M., Bauer F., First Results in thin film analysis based on a new EDS software to determine composition and/or thickness of thin layers on subsrates, EMC 2008 Vol 1, Springler-Verlag Berlin 2008, p 751,752

[24] Thermal Oxidation of Silicon, Professor Nathan Cheung, U.C. Berkeley EE143 Lecture # 5, http://www.eng.tau.ac.il/~yosish/courses/vlsi1/I-4-1-Oxidation.pdf , last accessed date: 13/09/2010

[25] Calculator Code by Eric Perozziello, Silicon Thermal Oxide Calculator http://www.lelandstanfordjunior.com/thermaloxide.html, last accessed date: 13/09/2010

[26] EDX depth profiling by means of effective layers
Kyaw Myint, T. Barfels, J.-C. Kuhr and H.-J. Fitting, Fresenius' Journal of Analytical Chemistry , 1998

[27] Dominique Drouin, Ph.D., B. Ing. , Supervisor, Website On CASINO Software, http://www.gel.usherbrooke.ca/casino/What.html , last accessed date: 13/09/2010

[28] Dominique Drouin, Ph.D., B. Ing. , Supervisor, Website On CASINO Software, http://www.gel.usherbrooke.ca/casino/ , last accessed date: 13,09,2010

APPENDIX A

Table: Dry and wet oxidation rate chart of Silicon for different temperatures.

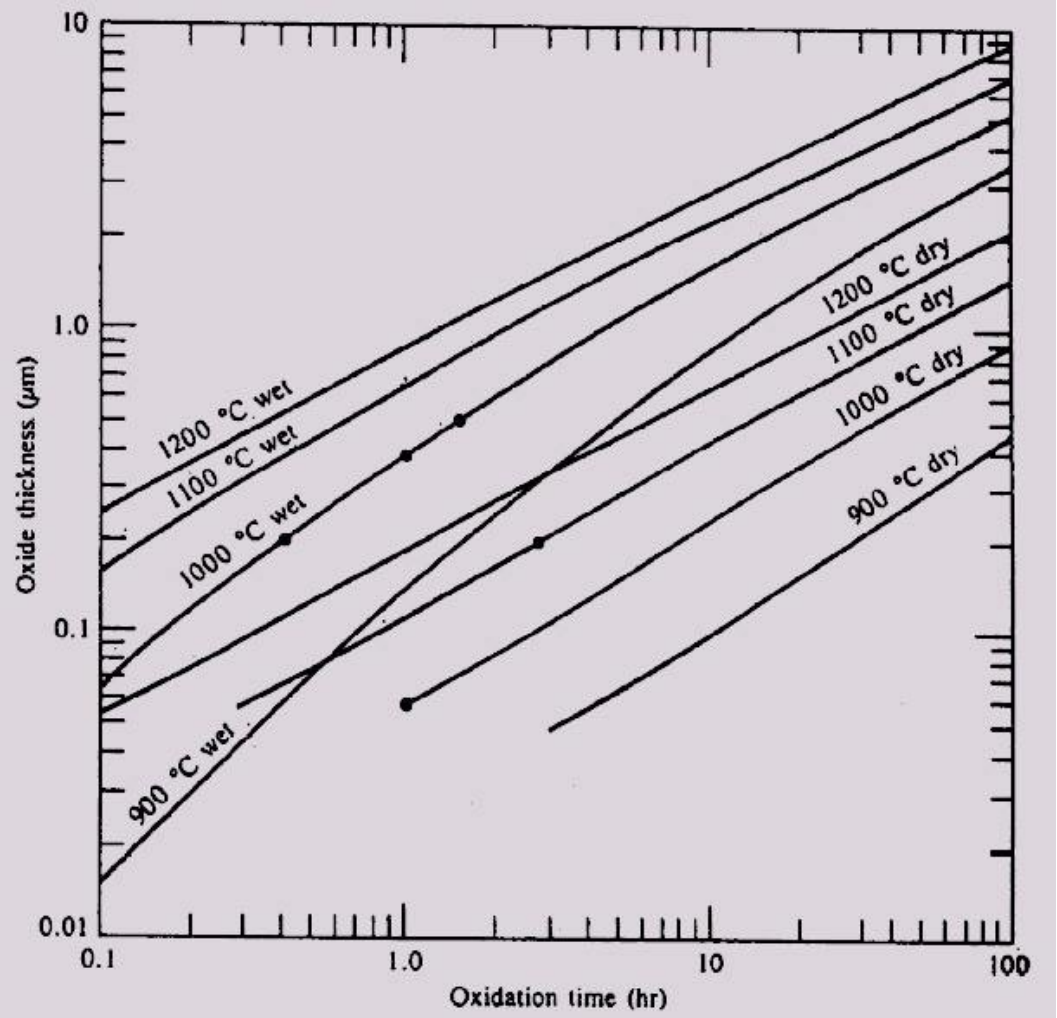

Wet and dry silicon dioxide growth for ⟨100⟩ silicon

APPENDIX B

Table: EDS gold ratio raw data of gold thin film on silicon substrate for different thicknesses at different SEM voltages

SEM Voltage (keV)	25nm	50nm	75nm	100nm	125nm	150nm	175nm	200nm
30	1,96	4,15	6,34	8,99	11,89	15,15	18,58	23,38
29	1,96	4,33	6,42	9,33	12,39	15,81	19,59	24,41
28	2,09	4,41	6,77	9,53	13,12	16,47	20,36	25,42
27	2,1	4,56	7,11	10,04	13,53	17,49	21,53	26,9
26	2,13	4,7	7,44	10,38	14,42	18,31	22,85	28,63
25	2,18	5,01	7,5	11,07	15,26	19,39	24,05	30,44
24	2,2	4,86	7,63	11,12	15,91	20,08	25,06	31,68
23	2,29	5,14	7,93	11,91	17,22	21,36	27,54	34,16
22	2,38	5,57	8,6	12,59	17,87	23,03	28,95	37,14
21	2,49	5,74	9,34	13,87	19,25	25,15	32,19	40,89
20	2,8	6,24	10,02	14,66	21,4	27,81	35,28	44,83
19	2,85	6,69	10,99	16,25	23,62	30,56	39,24	48,54
18	2,91	7,19	11,91	18,14	25,78	34,66	43,96	54,21
17	3,22	7,91	13,37	20,5	29,86	39,04	48,87	60,34
16	3,53	8,88	14,53	23,17	33,21	44,01	55,25	66,37
15	3,82	9,44	16,69	26,52	39,12	49,98	60,29	73,37
14	4,3	11,13	19,54	30,92	44,18	58,14	68,94	79,78
13	4,93	13,39	22,85	35,66	51,73	64,54	74,48	83,67
12	5,32	14,66	27,11	41,78	59,02	72,14	80,47	89,1
11	6,61	18,01	32,34	49,44	67,9	79,1	89,27	92,98
10	7,32	22,39	39,6	59,76	77,24	85,1	93,37	94,2
9	9,96	27,62	49,73	70,47	85,21	91,8	96,76	
8	12,88	36,83	61,95	80,48	90	93,46		
7	18,01	49,98	74,88	87,75	96,13			
6	26,15	63,77	85,63	92,1	97,58			
5	39,54	80,89	91,44	96,11				
4	61,57	88,96	95,59					
3	87	90,28	95,84					

APPENDIX C

Table: EDS germanium ratio raw data of germanium thin film on silicon substrate for different thicknesses at different SEM voltages

Voltage (keV)	25 nm	50 nm	75 nm	100 nm	125 nm	150 nm	175 nm	200 nm
30	0,88	1,37	1,89	2,63	3,35	4,12	4,83	5,93
29	0,87	1,52	1,99	2,67	3,67	4,23	5,15	6,07
28	0,65	1,28	2,04	2,95	3,67	4,36	5,25	6,42
27	0,7	1,4	2,06	2,87	3,92	4,53	5,44	6,57
26	0,73	1,4	2,22	3,02	3,92	4,91	5,73	7,03
25	0,65	1,36	2,26	3,13	4,27	4,94	6,12	7,44
24	0,92	1,54	2,66	3,6	4,72	5,59	7,2	8,34
23	0,93	1,6	2,79	3,86	4,93	5,97	7,37	8,96
22	0,96	1,79	2,95	3,96	5,33	6,39	7,84	9,88
21	1,06	1,81	3,16	4,32	5,74	7,04	8,33	10,69
20	1,01	2,07	3,3	4,53	6,01	7,21	9,09	11,14
19	1,03	2,06	3,47	5,14	6,55	7,84	9,99	12,24
18	1,2	2,26	3,67	5,58	7,24	8,92	10,63	13,79
17	1,2	2,53	4,1	6,17	8,14	9,88	11,65	15,45
16	1,3	2,82	4,57	6,62	9,2	10,8	13,76	16,79
15	1,32	3,13	5,01	7,61	10,01	12,58	15,62	19,37
14	1,65	3,58	6,35	9,12	12,12	15,26	18,63	23,25
13	1,96	4,35	7	10,14	13,97	17,29	21,58	27,65
12	2,08	4,87	8,33	12,01	16,64	20,55	26,01	32,68
11	2,71	5,74	10,4	14,58	20,46	25,45	31,01	40,26
10	3,28	7,34	12,37	18,03	24,76	30,61	38,5	48,02
9	3,54	8,96	16,33	22,47	31,15	39,54	47,33	57,72
8	4,69	11,17	20,17	30,4	40,78	49,96	59,9	70,58
7	6,46	15,01	27,62	39,88	52,67	64,92	73,2	81,92
6	8,79	21,32	37,87	53,73	70,43	78,73	85,81	91,05
5	12,62	33,95	56,18	73,6	85,45	90,79	94,83	96,13
4	22,48	52,76	79,72	90,06	94,41	96,8	98,27	
3	45,55	82,21	95,31	100	100	100	100	
2,5	65,76							
2	81,46							

APPENDIX D

Table: EDS aluminum ratio raw data of aluminum thin film on silicon substrate for different thicknesses at different SEM voltages

Voltage(keV)	50 nm	100 nm	150 nm	200 nm	250 nm	300 nm	350 nm	400 nm
30	1,87	2,69	4,1	5,3	7,41	8,17	9,95	11,69
29	1,79	2,88	4,32	5,87	7,46	8,74	10,37	12,08
28	1,91	3,02	4,19	6,09	7,63	9,23	10,53	12,28
27	1,79	3,14	4,48	6,08	7,84	9,6	11,15	12,87
26	2,11	3,1	4,58	6,6	8,37	9,8	11,77	13,51
25	2	3,23	4,88	6,78	8,65	10,38	11,91	14,18
24	2,22	3,29	5,22	7,58	9,71	11,71	13,59	15,75
23	2,22	3,51	6,03	8,4	10,11	11,98	14,63	16,96
22	2,37	3,66	5,79	8,69	10,87	13,01	15,34	17,72
21	2,54	3,84	6,12	9,32	11,92	14,05	16,48	19,48
20	2,51	4,19	6,52	9,74	12,74	14,89	17,72	20,58
19	2,62	4,42	7,14	10,55	13,31	16,27	19,25	22,75
18	2,96	4,58	7,66	11,32	14,85	17,48	20,99	24,47
17	2,79	5,37	8,61	12,39	16,11	19,58	22,77	26,63
16	3,39	5,66	9,31	13,54	17,94	22,02	25,52	30,73
15	3,6	6,31	10,44	15,18	19,85	23,75	28,36	33,63
14	3,58	6,87	11,33	16,36	21,86	26,25	31,15	36,2
13	3,99	7,64	12,44	18,83	24,68	29,94	35,24	40,54
12	4,62	8,99	15,49	22,95	29,56	36,61	42,24	48,7
11	5,81	10,82	18,14	26,89	34,48	42,99	49,65	56,12
10	6,31	12,69	21,16	31,96	41,78	50,98	57,53	64,71
9	7,36	15,88	27,01	39,02	50,39	58,32	66,73	75,21
8	9,39	20,68	33,33	48,84	61,26	69,48	77,81	85,19
7	11,71	26,16	43,41	59,92	73,99	82,01	88,16	92,5
6	15,44	35,4	57,19	75,08	86,4	93,4	96,22	98,27
5	20,72	49,99	74,34	89,77	95,73	98,21	99,3	99,36
4	34,27	71,13	92,57	98,1				
3	61,85	94,43	98,98					

APPENDIX E

Table: EDS oxygen ratio raw data of SiO_2 thin film on silicon substrate for different thicknesses at different SEM voltages

Voltage (keV)	50 nm	100 nm	150 nm	200 nm	250 nm	300 nm	350 nm	400 nm
30	7,28	12	15,84	18,65	20,72	23,59	25,08	28,08
29	8,02	12,13	15,57	20,44	21,92	24,87	26,19	29,9
28	8,06	11,68	14,93	18,86	22,86	24,07	26,72	28,23
27	8,23	12,31	14,81	20,13	22,32	24,83	27,08	29
26	8,2	12,96	15,39	19,78	22,42	24,95	26,52	29,42
25	7,45	12,41	14,73	20,7	22,94	24,71	26,75	29,79
24	8,94	15,02	18,04	21,76	24,83	26,77	29,43	32,92
23	9,56	14,44	17,54	22,84	24,78	27,61	30	32,84
22	9,18	14,06	17,48	22,77	25,4	27,52	29,56	33,77
21	9,63	15,17	18,16	24,28	26,19	28,34	31,14	33,18
20	9,34	14,51	17,51	23,96	25,74	28,86	31,41	35,26
19	9,66	15,13	17,71	24,68	26,76	29,66	30,87	35,49
18	9,64	15,66	20,04	24,67	26,94	29,19	32,65	36,35
17	9,76	15,77	18,68	24,06	26,31	30,59	32,8	36,37
16	10,61	16,33	18,73	23,8	27,54	30,82	33,91	38,1
15	10,56	15,55	18,91	25,99	28,41	31,44	33,82	38,73
14	9,52	15,72	18,45	24,11	27,98	31,7	34,01	38,11
13	9,57	15,45	19,68	25,62	29,2	32,38	36,04	40,61
12	11,01	18,22	22,84	28,42	33,14	36,38	40,91	45,23
11	13,88	19,22	23,41	30,6	34,5	38,95	42,45	47,98
10	14,02	21,03	26,6	32,66	38,34	42,84	45,48	50,27
9	14,53	22,1	28,11	36,24	41	44,52	49,48	54,61
8	17,4	25,32	29,59	39,87	45,11	48,95	53,31	58,47
7	19,49	29,33	36,54	47,12	50,75	55,51	58,25	64,29
6	22,11	34,06	41,6	53,3	57	60,72	63,56	66,36
5	29,07	42,42	52,33	59,6	64,71	65,35	67,3	67,91
4	38,33	54,75	62,91	66,38	67,54	67,64	68,02	
3	45,45	61,91	65,2	66,41				
2,5	54,74	64,01	65,39					